Geosystems and Geoenvironment 2 (2023) 100124

Contents lists available at ScienceDirect

Geosystems and Geoenvironment

journal homepage: www.elsevier.com/locate/geogeo

Paleoclimate evolution of the North Pacific Ocean during the late Quaternary: Progress and challenges

Yi Zhong[a], Zhengyao Lu[b], David J. Wilson[c], Debo Zhao[d], Yanguang Liu[e], Ting Chen[f], Congcong Gai[a], Xun Gong[g], Zhaoxia Jiang[h], Jiabo Liu[a], Qingsong Liu[a,i,j,*]

[a] *Center for Marine Magnetism (CM²), Department of Ocean Science and Engineering, Southern University of Science and Technology, Shenzhen 518055, China*
[b] *Department of Physical Geography and Ecosystem Science, Lund University, Lund, Sweden*
[c] *Institute of Earth and Planetary Sciences, University College London and Birkbeck, University of London, London, UK*
[d] *Key Laboratory of Marine Geology and Environment, Institute of Oceanology, Chinese Academy of Sciences, Qingdao, China*
[e] *Key Laboratory of Marine Geology and Metallogeny, First Institute of Oceanography, Ministry of Natural Resources (MNR), Qingdao, China*
[f] *Chongqing Key Laboratory of Wetland Science Research of the Upper Yangtze River, Chongqing Normal University, Chongqing, China*
[g] *Hubei Key Laboratory of Marine Geological Resources, China University of Geosciences (Wuhan), Wuhan, China*
[h] *Frontiers science Center for Deep Ocean Multispheres and Earth System, Key Lab of Submarine Geosciences and Prospecting Techniques, Ministry of Education, College of Marine Geosciences, Ocean University of China, Qingdao 266100, China*
[i] *Southern Marine Science and Engineering Guangdong Laboratory (Guangzhou), Guangzhou, China*
[j] *Shanghai Sheshan National Geophysical Observatory, Shanghai, China*

ARTICLE INFO

Article history:
Received 26 April 2022
Revised 15 July 2022
Accepted 19 August 2022

Handling Editor: Sanzhong Li

Keywords:
Paleoclimate evolution
Atmospheric circulation
Intermediate water formation
High-low latitude connections
Data-model comparison
North Pacific Ocean

ABSTRACT

High- and low-latitude climatic processes in the North Pacific Ocean are important components of the global climate system. For example, the interplay among North Pacific atmospheric circulation, ocean circulation, and biological productivity affects atmospheric carbon dioxide levels and marine oxygen concentrations. Here we review recent research on the North Pacific paleoclimatic and paleoceanographic evolution during the late Quaternary and its response to external forcings such as orbital insolation, ice-sheet extent, and greenhouse gas concentrations. First, we summarize the principles and application of relative paleointensity as a critical chronological tool in North Pacific paleoclimate research. Second, we illustrate the latest discoveries on the interaction between North Pacific Intermediate Water formation and high-to-low latitude teleconnection processes. Third, recent progress in linking dust fluxes and marine productivity and their global significance for the carbon cycle are presented. Finally, several key scientific problems are highlighted for future research on ocean-atmosphere-climate interactions in the North Pacific, pointing to the importance of combining paleo-records and modeling simulations. Overall, this review also aims to provide a broad insight into possible future changes of ocean-atmosphere circulation in the North Pacific region under a rapidly warming climate.

Contents

Abbreviations: NPO, North Pacific Ocean; PDW, Pacific Deep Water; NPIW, North Pacific Intermediate Water; EASM, East Asian Summer Monsoon; RPI, relative paleointensity; ENSO, El Niño-Southern Oscillation; LCDM, Lower Circumpolar Deep Water; UCDW, Upper Circumpolar Deep Water; NPDW, North Pacific Deep Water.

* Corresponding author.
E-mail address: qsliu@sustech.edu.cn (Q. Liu).

https://doi.org/10.1016/j.geogeo.2022.100124

1. Introduction

The North Pacific Ocean (NPO) is a terminus in the modern routing of the deep ocean currents of the global thermohaline circulation, which transports heat and salt within and between ocean basins (Lyle et al., 2008). Furthermore, Pacific Deep Water (PDW) constitutes a major reservoir for carbon and is important for carbon exchange between the ocean and the atmosphere due to the accumulation of the products of re-mineralized organic matter along deep-water flow pathways (Jaccard et al., 2009). Consequently, studies of the NPO paleoclimate evolution and paleoceanography could shed light on how distinct Earth systems respond and interact under varying global climatic boundary conditions.

The modern North Pacific is permanently capped by a freshwater lid, which constrains the large-scale sinking of surface water to the upper few hundred meters of the water column (Emile-Geay et al., 2003). Although synchronous changes have been reported between atmospheric CO_2 variability and oceanic export production in this region (Crusius et al., 2004; Galbraith et al., 2007; Gray et al., 2018; Rae et al., 2014, 2020), explanations for this coherent variation remain debated. For example, it could arise from some combination of changes in iron supply (Praetorius et al., 2015), water column stratification (Lam et al., 2013), or the formation and extent of glacial North Pacific Intermediate Water (NPIW) (Knudson and Ravelo, 2015, 2016). During glacial periods, enhanced dust fluxes to the region could have alleviated iron limitation (Martin, 1990), whereas reduced exchange between the surface and deeper waters could have led to a decrease in nutrient supply (Jaccard et al., 2005). Given the multiple possible controls and responses in this system, obtaining a better understanding will require improved constraints on ocean circulation and dust dynamics in the North Pacific over a range of timescales.

A key oceanographic feature of the NPO is the Kuroshio Current (Fig. 1), which strongly influences East Asian and global climates through ocean-atmosphere interactions between high- and low-latitude climate systems (Jaccard et al., 2005). On the one hand, the Arctic Oscillation and the Siberian High/Aleutian Low systems (Fig. 1a) are dominant factors controlling the amount of snow cover and winter strength, including the timing of sea-ice onset and breakup (Wu and Wang, 2002). Furthermore, these systems offer a connection between the high latitudes in the Atlantic and Pacific realms. On the other hand, during the summer, the East Asian Summer Monsoon (EASM) system transports moisture and heat from the tropics to the extratropical Pacific Ocean and also delivers precipitation to the major river drainage basins in the continental hinterland (Lembke-jene et al., 2018; Fig. 1a). In turn, variability in the freshwater release may play an important role in controlling sea-ice coverage and upper-ocean stratification (Okazaki et al., 2010; Riethdorf et al., 2013).

Apart from palaeoceanographic studies on the ocean dynamics in the NPO, source-to-sink studies from the Asian mainland to the Pacific Ocean have become an important frontier field in contemporary geoscience research. As the second-largest dust source on Earth, the arid and semi-arid areas in central Asia supply about 70

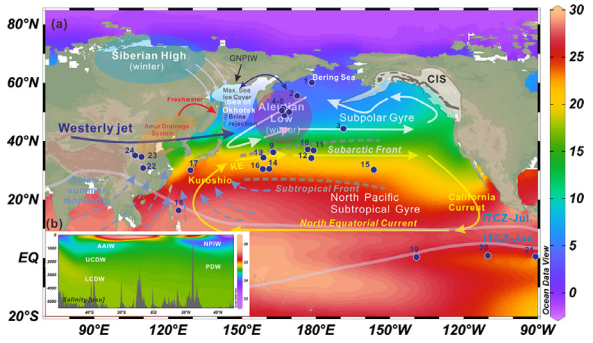

Fig. 1. (a) Ocean and atmospheric circulation in the North Pacific Ocean. The major ocean currents are based on Brown et al. (2001). Location of the Westerly Jet is based on Zhang and Huang (2011). Other atmospheric systems are shown schematically. Ocean temperatures (scale to right) are from the World Ocean Atlas 2013 (Locarnini et al., 2013), drawn with Ocean Data View software (Schlitzer, 2015). The glacial extent of the Cordilleran Ice sheet (CIS) is also shown. Locations of ocean drilling sites and cave sites referred to in the text are marked with blue labelled circles. ITCZ, intertropical convergence zone. (b) Modern seawater salinity profile along the Pacific meridional transect, based on the World Ocean Atlas 2013 (Locarnini et al., 2013). AAIW = Antarctic Intermediate Water, NPIW = North Pacific Intermediate Water, UCDW = Upper Circumpolar Deep Water, LCDW = Lower Circumpolar Deep Water, PDW = Pacific Deep Water. Detailed information of these sites is presented in Table 1.

Mt of dust to the NPO every year, which is carried by the westerly winds and the East Asian Winter Monsoon (Shao et al., 2011; Fig. 1a). Such eolian dust input may be a significant factor controlling primary productivity in the North Pacific because it enhances the biological pump efficiency (Buesseler et al., 2007; Han et al., 2011; Wan et al., 2020). However, the interaction between iron fertilization and biogeochemical cycles in the NPO remains unclear (Chen et al., 2020; Jacobel et al., 2019; Winckler et al., 2016).

For a long time, the application of oxygen isotope stratigraphy and radiocarbon dating of sediments based on calcareous microfossils was not widely available for most of the NPO. In addition, research into these systems, including atmospheric and ocean circulation, dust inputs, and productivity, was generally conducted independently. Consequently, while their importance for the global carbon cycle is recognized, the relationships between these North Pacific climate systems over different spatio-temporal scales are not always clear. In this contribution, we focus on recent progress that has been made in understanding these NPO systems, both individually and in terms of the interactions between them during the late Quaternary (Fig. 1 and Table 1). After introducing the modern atmospheric and ocean circulation in this region, we first analyze the key role of relative paleointensity (RPI) studies in developing North Pacific age models. Second, we review recent evidence for changes in NPIW formation and developments in understanding its forcing mechanisms. Third, we address the controls on Asian dust inputs and NPO paleo-productivity, and their links to CO_2 regulation. We conclude by discussing the need to combine data and modeling approaches to understand the climatic systems of the North Pacific and consider the significance of this region for the global carbon cycle.

Table 1
Lists of paleoclimatic records in North Pacific Ocean and East Asia.

Num	Area	Sites	Latitude	Longitude	Water depth (m)	References
1	Bering Sea	U1345	60°9′N	179°28′W	1008	Jang et al., 2017
2	Bering Sea	U1342	53°33.4′N	176°49.0′E	1950	Worne et al., 2019
3	Subarctic Pacific Ocean	ODP Site 885	44°41.3′N	168°16.0′E	5711	Rea et al., 1998; Zhang et al., 2020a, 2020b
4	Subarctic Pacific Ocean	ODP Site 882	50°21′	167°35′E	3244	Serno et al., 2017
5	Subarctic Pacific Ocean	LV76–18	49.05°N	168.55°E	2863	Cheng et al., 2022
6	Subarctic Pacific Ocean	ES	49°44.70′N	168°18.93′E	2388	Tanaka and Takahashi, 2005
7	Subarctic Pacific Ocean	LV63–4–2	51.63°N	167.81°E	2946	Zhong et al., 2021
8	Subarctic Pacific Ocean	ODP 883	51°11.9′N	167°46.1′E	2385	Roberts et al., 1997
9	Mid-latitude Pacific Ocean	V21–126	37°41′N	163°02′E	3968	Hovan et al., 1989
10	Mid-latitude Pacific Ocean	SO202–37–2	37°46.07′	176°16.13′	3658	You et al., 2018
11	Mid-latitude Pacific Ocean	KK75–02	38°37.4′N	179°19.7′E	5475	Janecek and Rea, 1985
12	Mid-latitude Pacific Ocean	H3571	34°54.25′N	179°42.18′E	3571	Kawahata et al., 2000
13	Mid-latitude Pacific Ocean	NGC108	36°36.9′N	158°20.9′E	3390	Maeda et al., 2002
14	Mid-latitude Pacific Ocean	ODP Site 576	32°21.4′N	164°16.5′E	6220	Janecek, 1985
15	MMid-latitude Pacific Ocean	LL44-GPC3	30°19.4′N	157°49.4′W	5705	Janecek and Rea, 1985
16	Mid-latitude Pacific Ocean	ODP Site 1209B	32.65°N	158.50°E	2387.2	Zhang et al., 2019
17	Japan Sea	U1429	31°37.04′N	128°59.85′E	732	Zhao et al., 2021
18	Philippine Sea	MD06–3047	17°00.44′N	124°47.93′E	2510	Xu et al., 2015
19	Equatorial Pacific Ocean	TT013-PC72	0.1°N	139.4°W	4298	Winckler et al., 2008
20	Equatorial Pacific Ocean	ODP Site 849	0°11′N	110.5°W	3851	Winckler et al., 2016
21	Equatorial Pacific Ocean	ODP Site 1240	0.02°N	86.46°W	2921	Jacobel et al., 2019
22	Central China	Sanbao Cave	31°40′N	110°26′E	1900	Cheng et al., 2016
23	Central China	Luochuan	35.8°N	109.4°E	–	Han et al., 2020
24	Central China	Xifeng	35.75°N	107.82°E	–	Guo et al., 2009

2. Oceanographic setting

The NPO is a vast region that is influenced by both high- and low-latitude climate systems, making it a vital setting in which to understand both polar and tropical climate mechanisms and the coupling between them (Lohmann et al., 2019). It is subdivided into the Subpolar Gyre and the North Pacific Subtropical Gyre by the Subarctic Front (Fig. 1a; Qiu, 2002). The Subarctic Front, located between 40°N and 44°N in the central North Pacific, is characterized by an abrupt change in temperature and salinity where the warm and salty subtropical water from the south meets the cold and freshwater of the Subpolar Gyre to the north (Yuan and Talley, 1996).

The northern sector of the North Pacific open ocean and the subarctic marginal seas are characterized by the annual onset and breakup of sea ice, with the timing mainly controlled by the Arctic Oscillation and the winter strength of the Siberian High/Aleutian Low system (Batchelor et al., 2019; Fig. 1a). The southern sector of the NPO is more strongly dominated by the low latitude EASM and El Niño-Southern Oscillation (ENSO) systems (Ding et al., 2014; Liu et al., 2014). The EASM and ENSO systems transfer moisture and heat from the tropics to the extratropics during summer and winter, respectively. In addition, the baroclinic instability of the westerly jet shapes the North Pacific storm tracks, which shift together with westerly jet movement and represent the main forcing for mid-latitude rainfall (Graff and LaCasce, 2012; Shaw et al., 2016). Both the precipitation over the ocean and the riverine freshwater discharge (from precipitation over the continent) play a role in the upper ocean hydrography, such as the formation of NPIW.

Dramatic variations in climatic boundary conditions impacted the NPO during the glacial-interglacial cycles of the Quaternary period. At high latitudes, the periodic advance and retreat of Northern Hemisphere ice sheets took place every ~100 kyr (Hays et al., 1976; Lu et al., 2019a). Those changes were accompanied by fluctuations in the strength of the Aleutian Low (Zhong et al., 2021), which were also partly influenced by remote forcing from western equatorial Pacific precipitation (Maier et al., 2018). The Aleutian Low further modulated sea-ice distributions in the Bering Sea and the Sea of Okhotsk (Cavalieri and Parkinson, 1987) and impacted intermediate water production in both marginal seas (Kender et al., 2019; Khim et al., 2012). In the extratropics, the EASM pattern and/or intensity changed on orbital timescales, with a control by orbital forcing (particularly precession) evident in Chinese cave speleothem records (Cheng et al., 2016; Wang et al., 2008), while other monsoon proxy records indicate a stronger forcing by global ice volume (Liu et al., 2020). In the tropics, the evolution of ENSO followed prominent precession cycles during the late Quaternary period (Lu and Liu, 2019; Lu et al., 2019b), with the amplitude linked to the strength of the ocean-atmosphere feedbacks in the tropical Pacific in response to orbital forcing (Lu and Liu, 2018). The ENSO and EASM systems in the North Pacific were synchronized over orbital timescales via atmospheric teleconnections (Lu et al., 2019b). In addition, climate proxy data indicate that local intrinsic climate variability, such as Pacific decadal variability, also affected the North Pacific climate (D'Arrigo et al., 2005).

Due to a lack of deep-water formation in the modern subarctic Pacific (Warren, 1983), the deep North Pacific is slowly replenished by a mixture of waters from Southern Ocean that first originated as the North Atlantic Deep Water and Antarctic Bottom Water from (Talley, 2013). Specifically, PDW consists of Lower Circumpolar Deep Water (LCDW) and Upper Circumpolar Deep Water (UCDW), which flow northward into the central Pacific Ocean Basin (Fig. 1b). North Pacific Deep Water (NPDW) originates from vertical mixing of LCDW with the subsurface water masses of the North Pacific (Kawabe and Fujio, 2010). Therefore, the deep North Pacific contains the oldest and most CO_2-enriched water masses in the modern open ocean (Broecker et al., 2004).

NPIW is the densest water mass at a water depth between ~300–800 m in the modern NPO (Talley, 2003). It is sourced from the Sea of Okhotsk during winter-time sea-ice formation when brine production occurs on the continental shelf within coastal polynyas (Shcherbina et al., 2003). Millennial and glacial-interglacial changes in NPIW formation have been inferred during the Quaternary period, and a variety of mechanisms have been put forward to explain them, including changes in sea-ice volume (Worne et al., 2019), closure of the Bering Strait (Kender et al., 2018; Knudson and Ravelo, 2016), changes in the strength of the EASM and associated moisture and heat transport (Lembke-Jene et al., 2018), and the exchange of saline water between the subtropical and subpolar gyres (Gong et al., 2019). During the

last glacial period, the Bering Sea became a potential additional source of NPIW, leading to enhanced ventilation of the Pacific Ocean (Horikawa et al., 2010; Rella et al., 2012; Tanaka and Takahashi, 2005; Zhong et al., 2021). Such an expansion of glacial NPIW would have actted to enhance stratification throughout the NPO, impacting vertical mixing, nutrient supply, and the biological pump (Worne et al., 2019; Ovsepyan et al., 2021).

3. Quaternary geochronology in the north pacific ocean

Precise and accurate chronologies are a crucial prerequisite for paleoceanographic studies and set a baseline for the resolution that may potentially be achieved when comparing or correlating between different marine records, or between marine, terrestrial, and ice core records (Channell et al., 2020; Lane et al., 2017). Because most of the deep seafloor of the Pacific Ocean lies below the carbonate compensation depth (Roberts et al., 1997; Yamamoto et al., 2007; Yamazaki, 1999), carbonate dissolution restricts the availability of continuous planktonic and benthic foraminifera records, thereby hindering the use of the well-established oxygen isotope stratigraphy (Lisiecki and Raymo, 2005) or radiocarbon dating based on calcareous microfossils.

In the absence of carbonate sediments, Jaccard et al. (2005, 2010) used both Ba/Al ratios and biogenic opal records (Fig. 2b) to indicate the climate-related signal, with high values occuring during interglacial stages and lower values during glacial stages (Fig. 2a; Lisiecki and Raymo, 2005). On orbital timescales, eolian dust records in the NPO generally show a correlation with global ice volume (Fig. 2c; Winckler et al., 2008). Hence, Zhang et al. (2019) suggested that neodymium isotopes in the dust fraction of the sediments could be applied as a chronostratigraphic tool in this region. Notobly, low (unradiogenic) Nd isotope compositions at ODP Site 1209 on the Shatsky Rise (Fig. 2d; Zhang et al., 2019) and in core MD06–3047 from the western Philippine Basin (Fig. 2e; Xu et al., 2015) corresponded to high dust fluxes in the Pacific Ocean during glacial periods, as seen in core TT013-PC72 (Fig. 2c; Winckler et al., 2008). Over longer timescales, both magnetostratigraphy and $^{10}Be/^{9}Be$ dating were shown to provide insights for the geochronology of abyssal sedimentation in the Mariana Trench (Yi et al., 2020).

The above examples can represent useful stratigraphic tools for NPO sediments in specific cases, but suffer from several limitations, including spatial restrictions and a lack of temporal resolution. Instead, geomagnetic paleointensity analysis represents an alternative approach for generating independent age assignments for generating independent age assignments for Quaternary sedimentary records and for can facilitate inter-core and even interhemispheric correlation (Roberts, 2008). In particular, geomagnetic dipole intensity signals are globally consistent, so RPI records can be comparable in sediments from global sites (Roberts et al., 2013). Moreover, RPI records are insensitive to seawater chemistry (Roberts et al., 2013), which represents a benefit over oxygen isotope stratigraphy. A method to estimate sedimentary RPI was first proposed by Levi and Banerjee (1976), who normalized the natural remanent magnetization of sediments from Lake St. Croix with an artificial laboratory-induced magnetization (such as anhysteretic remanent magnetization or isothermal remanent magnetization), and found that the sedimentary RPI had the same general features as seen in paleomagnetic studies. More recently, the experimental and theoretical foundations for sedimentary RPI studies have been reviewed by Tauxe (1993) and Tauxe et al. (2006), and it should be noted that conventional criteria for RPI studies require that the magnetic carriers in sediment sequences are relatively homogeneous (King et al., 1983; Tauxe, 1993).

Paleomagnetic studies from the NPO and its marginal seas have progressed significantly in recent years (Gai et al., 2021; Shin et al., 2019; Wang et al., 2022). In Fig. 2, RPI records from the NPO are shown together with other global and regional records. The PISO-1500 (Channell et al., 2009) record (Fig. 2h) represents a global RPI stack, while the NOPAPIS-250 (Yamamoto et al., 2007) and NP02 records (Gai et al., 2021; Fig. 2f and g) reflect low-mid latitude RPI records from the North Pacific. High-latitude RPI records are represented by an RPI stack for the subarctic Pacific Ocean (Fig. 2i), which was calculated from ODP Sites 883/884 (Roberts et al., 1997), core LV63–4–2 (Zhong et al., 2020), Okhotsk Sea (Yamazaki et al., 2016), and Arctic Ocean records (Simon et al., 2016). Coherent variations between RPI records from the NPO and global stacks, as well as between the mid- and high-latitude regional records, can be expected to reflect dipolar geomagnetic variations (Yamazaki et al., 2016; Fig. 2f-i). Indeed, a general agreement between those regional and global RPI records is recognized, although age uncertainties limit comparisons between some of the records. Specifically, the RPI stack calculated here for the subarctic Pacific Ocean (Fig. 2i) demonstrates minima at ~41 ka (Laschamp excursion) and ~120 ka (Blake excursion). The broad similarity of

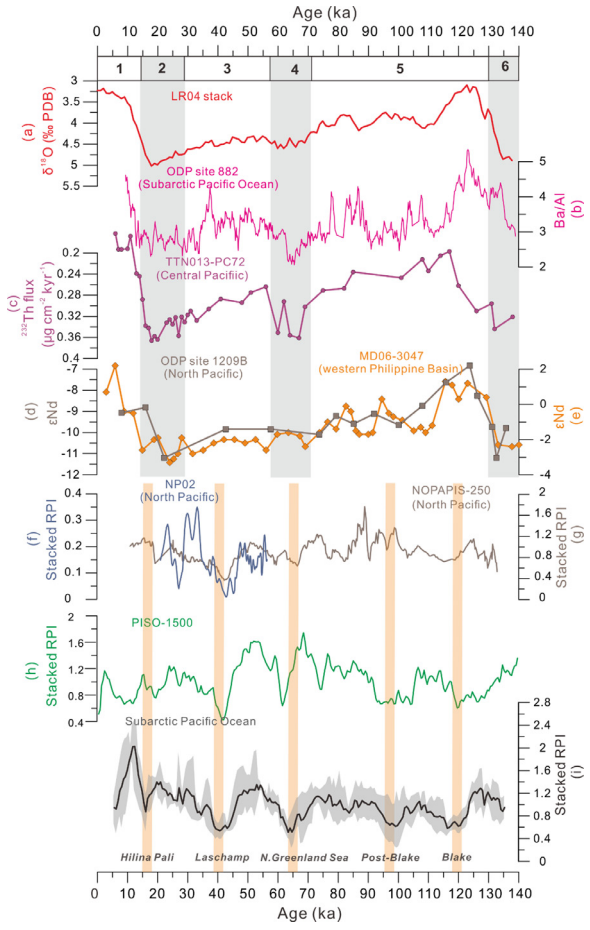

Fig. 2. Comparison of global and North Pacific Ocean paleoclimatic and paleomagnetic records: (a) LR04 benthic foraminiferal $\delta^{18}O$ stack (Lisiecki and Raymo, 2005); (b) Ba/Al ratios at ODP Site 882 (Jaccard et al., 2010); (c) ^{232}Th fluxes from core TT013-PC72 in the central equatorial Pacific (Winckler et al., 2008) (note the reversed axis); (d) dust-fraction Nd isotope evolutions at ODP Site 1209 (Zhang et al., 2019); (e) dust-fraction Nd isotope evolution in core MD06–3047 (Xu et al., 2015); (f) NP02 RPI stack records from the North Pacific (Gai et al., 2021); (g) NOPAPIS-250 RPI stack from the North Pacific (Yamamoto et al., 2007); (h) PISO-1500 RPI stack (Channell et al., 2009); (i) Subarctic Pacific Ocean RPI stack calculated here using data from ODP Sites 883/884 (Roberts et al., 1997), LV63–4–2 (Zhong et al., 2020), and Okhotsk Sea (Yamazaki et al., 2016) and Arctic Ocean records (Simon et al., 2016), and. Marine isotope stage (MIS) number are indicated along the top of the panel. gray bars indicate glacial periods and orange bars indicate the magnetic excursion events.

RPI behavior between different regions implies that, in first-order, the RPI variations are controlled by the geomagnetic dipole field (e.g., Roberts et al., 2013).

Although RPI-assisted chronologies have been used extensively in late Quaternary studies from the NPO since the 1990s (Gai et al., 2021; Kiefer et al., 2001; Roberts et al., 1997; Shin et al., 2019; Yamazaki, 1999), it is not always feasible to construct such chronologies in a given core. In contrast to the conventional requirement that magnetic carriers in sediment sequences are relatively homogeneous (King et al., 1983; Tauxe, 1993), NPO sediments usually consist of magnetic mineral components with different grain-size distributions (Yamazaki and Ioka, 1997a; Yamazaki and Shimono, 2013; Zhang et al., 2018). In such cases, it should be ensured that these components record consistent RPI variations (Gai et al., 2021). In addition, apart from the dominant dipole characteristics, a significant contribution from the non-dipole component of the geomagnetic field can sometimes be present, particularly during geomagnetic reversals and excursions (Leonhardt et al., 2009; Roberts, 2008; Zhong et al., 2020), which would complicate global and inter-regional RPI correlation. Furthermore, magnetic mineral diagenesis, which can alter the original sedimentary paleomagnetic signals, should always be taken into consideration in paleomagnetic studies (Roberts, 2015).

Two main challenges are that the geomagnetic field can have a non-dipolar geometry, such as during geomagnetic excursions (Roberts, 2008), and that regional geomagnetic characteristics can be smoothed during the construction of global stacks. Hence, chronological artifacts may occur when attempting to correlate a regional RPI record in the depth domain to a global RPI reference stack in the time domain. To better confrom fidelity of a constructed chronology, we should construct high-quality regional RPI reference stacks and combine the RPI approach with the independent dating methods where available to validate their consistency and reliability.

4. Progress in understanding the paleoclimate of the north pacific ocean

4.1. Influence of high-low latitude dynamics on North Pacific Intermediate Water

Reconstructing past changes in the formation and extent of NPIW is crucial for assessing its CO_2 storage capability and for constraining Pacific meridional heat transport, which are both important components of the global climate system (Sigman et al., 2010). During the last glacial period, evidence from deep-sea radiocarbon ventilation ages and benthic foraminiferal $\delta^{13}C$ records suggest changes in the mid-depth circulation (the upper ~1000–2000 m water depth) of the NPO, with enhanced intermediate water ventilation in the North Pacific and a more distinct mid-depth water mass boundary than today (Herguera et al., 1992; Matsumoto et al., 2002; Max et al., 2014, 2017; Okazaki et al., 2012). During the last deglaciation, NPIW may then have collapsed, enabling overturning to bring nutrient and CO_2-rich deep waters to the surface (Gray et al., 2018). However, reconstructions of sea-ice distribution and bottom-water ventilation, as well as sea-surface temperature and productivity records, are mostly only available for the last glacial cycle (Davis et al., 2020; Ovsepyan et al., 2021; Rae et al., 2020). Across multiple glacial-interglacial cycles, there is some evidence that high-latitude sea-ice formation and the associated NPIW formation could have regulated deep-water upwelling and ocean-atmospheric CO_2 exchange (Knudson and Ravelo, 2016; Leduc et al., 2010; Worne et al., 2019), but constraints on the forcing mechanisms of NPIW are lacking due to the scarcity of high-resolution records.

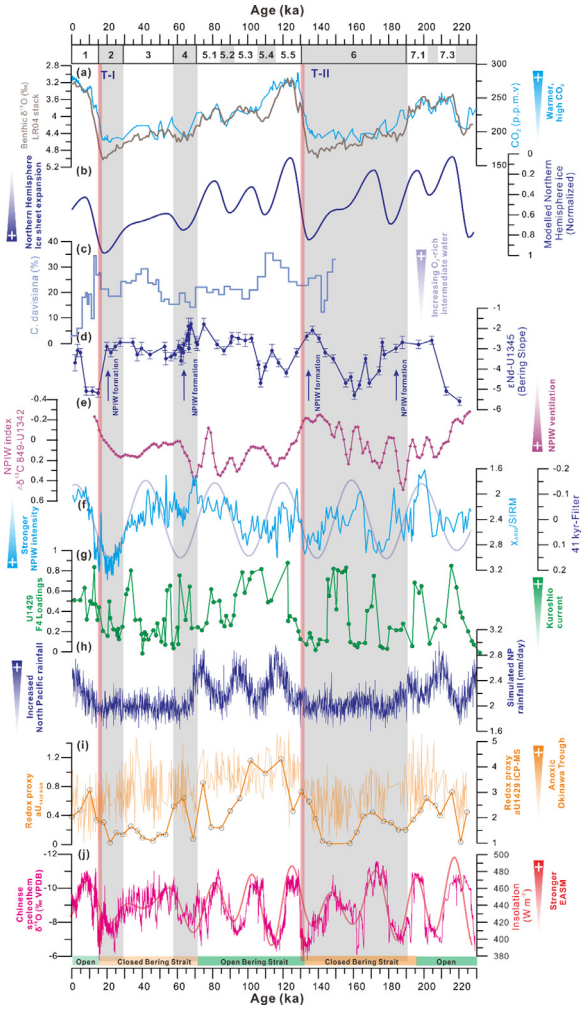

Fig. 3. North Pacific Intermediate Water (NPIW) evolution and forcing mechanisms since 230 ka. (a) LR04 benthic foraminiferal $\delta^{18}O$ stack (Lisiecki and Raymo, 2005) and atmospheric CO_2 concentration (Lüthi et al., 2008). (b) Modelled Northern Hemisphere ice volume (Bintanja et al., 2005). (c) Percent *Cycladophora davisiana* in Pacific core ES, as an indicator of intermediate water oxygenation (Tanaka and Takahashi, 2005). (d) Neodymium isotope (εNd) reconstruction from sediment leachates in Bering Sea core U1345, with more radiogenic values (arrows) interpreted to indicate NPIW formation in the Bering Sea (Horikawa et al., 2010; Jang et al., 2017). (e) Carbon isotope gradient ($\Delta\delta^{13}C_{849\text{-}U1342}$) between Pacific Ocean (ODP 849) and Bering Sea (U1342) cores, as a proxy for NPIW ventilation (Knudson and Ravelo, 2016). (f) χ_{ARM}/SIRM in core LV63–4–2 as an indicator of NPIW intensity, and 41 kyr Gaussian bandpass filtered output (thick blue line) (Zhong et al., 2021). (g) Factor-4 loadings of IODP Site U1429, as a proxy for Kuroshio Current strength (Vats et al., 2020). (h) Simulated North Pacific rainfall since 230 ka (Zhao et al., 2021). (i) Redox proxy of authigenic uranium (aU) based on natural gamma radiation (high-resolution record, left axis) and ICP-MS data (low-resolution record, right axis) at IODP Site U1429 (Zhao et al., 2021). (j) Chinese cave stalagmite $\delta^{18}O$ (Cheng et al., 2016) and Northern Hemisphere summer insolation (65° N, July-September; Laskar et al., 2004). EASM, East Asian Summer Monsoon. gray bars indicate glacial periods, and thick pink lines indicate glacial terminations (T-I and T-II). Conditions of an open or closed Bering Strait are indicated by coloured bars at the bottom of the panel. Marine isotope stage (MIS) numbers are indicated along the top of the panel.

Here, we have compiled multiple proxies from different regions of the North Pacific to assess the roles of high-latitude ice sheets (Lisiecki and Raymo, 2005; Fig. 3a) and low-latitude oceans (Cheng et al., 2016; Fig. 3j) in driving changes in NPIW formation through the last two glacial cycles. Many previous studies have emphasized the role of high-latitude climate on NPIW formation (e.g., Costa et al., 2018; Worne et al., 2019). Ice sheet growth (Bintanja et al., 2005; Fig. 3b) can affect NPIW circula-

tion by increasing land-surface albedo, lowering sea levels, and intensifying high-pressure atmospheric systems (Hu et al., 2010; Knudson and Ravelo, 2016). For example, intermediate waters were formed in the Bering Sea during glacial times, whereas today they mostly form only in the Sea of Okhotsk (Fig. 1), and this process played an important role in the formation of glacial NPIW (Horikawa et al., 2010; Tanaka and Takahashi, 2005). Specifically, evidence for cold and well-oxygenated intermediate waters in the glacial Bering Sea is provided by changes in radiolarian assemblages (Fig. 3c; Tanaka and Takahashi, 2005), while the sinking of local surface waters is evidenced by neodymium isotopes (Fig. 3d; Horikawa et al., 2010; Jang et al., 2017). The formation of glacial Bering Sea intermediate waters resulted from the expansion of the Laurentide ice sheet and the easterly-shifted Aleutian Low (Gong et al., 2019; Gray et al., 2018; Fig. 1). The shifts in this atmospheric system would have enhanced sea-ice formation and brine rejection, thereby increasing the salinity of cold surface waters, enabling their subduction to mid-depths in the Bering Sea, and providing an important precursor of glacial NPIW (Rella et al., 2012). Benthic foraminiferal $\delta^{13}C$ isotope records from the Bering Sea also support this process (Fig. 3e), and such records extend further back in time, providing evidence that enhanced glacial NPIW formation also occurred during previous extreme glacial intervals of the last 1.2 Myr (Knudson and Ravelo, 2016). Due to the complexity and specificity of NPIW proxies, studies in the subarctic North Pacific have provided crucial constraints on the source regions and extent of NPIW in the past, but further research is required into the forcing mechanisms on orbital timescales.

Magnetic minerals in marine sediments are useful proxies for tracing terrestrial sediment source areas and can also be applied to reconstruct water mass pathways, as illustrated by studies from the North Pacific (Korff et al., 2016; Shin et al., 2018; Zhang et al., 2018). Magnetic grain-size proxies and fabric alignment coefficients are particularly sensitive to deep-water flow dynamics and sedimentary changes (Kissel et al., 2009), with the direction and magnitude of anisotropy of magnetic susceptibility being widely used to reconstruct the azimuth and strength of paleo-flow (Kissel et al., 2013; Zheng et al., 2016; Nichols et al., 2020). During the last two glacial cycles, a significant 41-kyr periodicity was recorded in the magnetic mineralogy in core LV63–4–2 from the subarctic Pacific Ocean (Fig. 3f; Zhong et al., 2021). The intervals with finer magnetic grain size reflected the effects of intensified brine rejection and NPIW ventilation in the Bering Sea and the Sea of Okhotsk (Fig. 3d; Jang et al., 2017). Apart from the orbital-scale variability in NPIW formation, changes in the direction of anisotropy of magnetic susceptibility between different glacial periods suggest that shifts in the Aleutian Low could have controlled the source of NPIW formation between the different marginal seas (Zhong et al., 2021). Overall, this coupled ocean-atmosphere system represents a potential amplifier of climate variability that operates by controlling the sea-ice extent and NPIW formation in the marginal seas.

Outside of the high latitudes, the low-latitude surface ocean holds large amounts of heat and fresh water, such that its poleward transport was proposed to contribute to the upper ocean stratification and thereby limit subsurface ventilation during the last glacial termination in the subarctic Pacific Ocean (Okazaki et al., 2010). Specifically, the western boundary currents in the Northern Hemisphere could supply heat and fresh water from the low-latitude ocean to the northern middle and high latitudes, coupled with North Pacific storm tracks (Hu et al., 2015). Modern observations (Yang et al., 2020) and climate simulations (Sakamoto et al., 2005) suggest that global warming leads to a strengthening and poleward shift of the Kuroshio Current. The Kuroshio species (Fig. 3g; Vats et al., 2020) and EASM intensity (Fig. 3j; Cheng et al., 2016) were stronger during the interglacial periods, and display a periodicity of 23 kyr, indicating a precession signal. These orbital-scale dynamics of the Kuroshio Current are controlled by tropical atmosphere-ocean interactions, which could therefore influence atmospheric water vapor transport in the extratropical region (Zou et al., 2021).

In the above context, the anti-phased relationship between the NPIW intensity (Fig. 3f) and the EASM evolution (Fig. 3j) indicates that the low-latitude water vapor transport could play some role in influencing NPIW ventilation. Simulated North Pacific net rainfall (Fig. 3h) shows a similar pattern to redox variations in Site U1429 from Okinawa Trough (Fig. 3i), with increased net rainfall corresponding to weakened NPIW formation (Fig. 3e; Zhao et al., 2021). Increases in net rainfall could lead to freshening of the NPIW formation area, thereby controlling the North Pacific surface and intermediate ocean hydrography, and increasing vertical ocean stratification. Under global warming, several components of the large-scale extratropical atmospheric circulation are expected to change, including poleward shifts of the westerly winds (Chiang et al., 2015), jet streams (Kong and Chiang, 2020), storm tracks (Shaw et al., 2016), and the pattern of precipitation (Scheff and Frierson, 2012). Such poleward shifts of the extratropical circulation can be expected to impact ocean heat transport, net rainfall, and ocean circulation, and could therefore contribute, in addition to high latitude forcings, to a weakening or collapse of NPIW.

4.2. Asian dust dynamics recorded in the North Pacific Ocean

Understanding how the eolian dust cycle in the NPO interacts with the climate system has become an increasingly hot topic in recent years (Jickells et al., 2005; Jacobel et al., 2019). Previous studies have systematically explored the source-to-sink fluctuations of eolian dust using multiple mineralogical, geochemical, and isotopic tracers (e.g., Sun et al., 2019). Constraints on past changes in such source-to-sink processes shed light on the paleoclimate evolution in the Asian interior, as well as the evolutionary history of the Northern Hemisphere westerlies (Rea et al., 1998; Shen et al., 2017). Specifically, both tectonic- and climate-induced changes in the source regions (e.g., tectonic uplift and aridity) and atmospheric circulation patterns (e.g., the westerlies and winter monsoon) can lead to temporal variations in dust transport, in terms of both fluxes and provenance (Yan et al., 2017; Zhang et al., 2018).

Most eolian dust records from the NPO have been generated on distal open-ocean sediment cores, such as LL44-GPC3, DSDP Site 576, and ODP 885/886, which provide evidence for processes such as Asian drying, Tibetan uplift, and Northern Hemisphere cooling (Rea et al., 1998; Zhang et al., 2020b). For example, evidence can be obtained on both the eolian dust flux and grain size, which are similar between core LL44-GPC3 and DSDP Site 576 (Janecek, 1985; Janecek and Rea, 1983). Over long timescales, increases in eolian dust flux in the late Oligocene, the middle Miocene, and the late Pliocene to Pleistocene may reflect the tectonic movement of the core sites into the domain of the westerly winds, enhanced aridity linked to global cooling, and the Plio-Pleistocene onset of Northern Hemisphere Glaciation (Janecek, 1985; Janecek and Rea, 1983). In addition, weathering processes in the Asian dust source regions and climate-forced migration of the westerly winds probably also influenced the Asian eolian dust fluxes to the NPO since the late Pliocene (Abell et al., 2021; Zhang et al., 2020a).

To obtain the eolian dust signal from a marine sediment core, many of those studies used a chemical leaching method (Rea and Janecek, 1981). Other approaches used in the NPO include quartz separation (Wan et al., 2007), elemental analysis (Anderson et al., 2019; Kyte et al., 1993; Weber et al., 1996; Ziegler and Murray, 2007), clay minerals (Shen et al., 2017), helium isotopes (Abell et al., 2021; Patterson et al., 1999; Serno et al., 2017), and

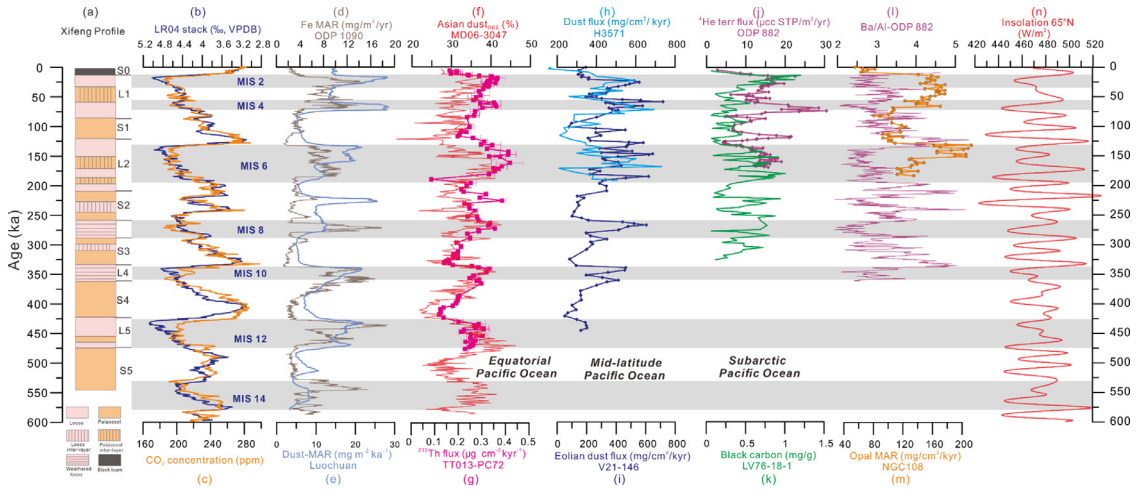

Fig. 4. Eolian dust records from the Chinese Loess Plateau and Pacific Ocean since 600 ka. (a) Loess-paleosol records in the Xifeng profile (Guo et al., 2009; lables S and L represent sapropel and loess layers, respectively); (b) LR04 benthic $\delta^{18}O$ stack (Lisiecki and Raymo, 2005); (c) atmospheric CO_2 concentration from the Antarctic EPICA Dome C ice core (Luthi et al., 2008); (d) iron (Fe) MAR at ODP Site 1090 (Martínez-Garcia et al., 2011); (e) dust MAR for Luochuan (Han et al., 2020); (f) Eolian dust inputs estimated from rare earth elements in core MD06–3047 from the Philippine Sea (Xu et al., 2015); (g) ^{232}Th fluxes from core TT013-PC72 in the central equatorial Pacific (Winckler et al., 2008); (h) dust fluxes from core H3571 on Hess Rise (Kawahata et al., 2000); (i) dust fluxes from core V21–146 on Shatsky Rise (Hovan et al., 1991); (j) ^{230}Th-normalized $^{4}He_{terr}$ flux from ODP Site 882 (Serno et al., 2017); (k) black carbon concentrations in core LV76–18 (Cheng et al., 2022); (l) Ba/Al ratios from ODP Site 882 (Jaccard et al., 2010); (m) opal MAR in core NGC108 (Maeda et al., 2002); (n) 65°N June insolation (Berger, 1978). gray bars indicate glacial periods, labelled with marine isotope stage (MIS) numbers.

environmental magnetism (Bailey et al., 2011; Doh et al., 1988; Yamazaki and Ioka, 1997b; Zhang et al., 2018). Multi-proxy comparison based on these different methods can aid validation and improve the accuracy and reliability of dust information obtained from marine sediments. Compared to tectonic timescales, our understanding of orbital-scale variability in eolian dust inputs to the NPO is limited by the scarcity of well-resolved records from this region. Furthermore, there is no compelling evidence for marine biological productivity changes between glacial and interglacial periods in the various domains of the NPO (i.e., subarctic Pacific, mid-latitude Pacific, and equatorial Pacific), whereas such evidence might have been anticipated as a response to changes in iron fertilization through atmospheric dust (Kienast et al., 2004).

High-resolution reconstructions of dust inputs to the low-latitude NPO over orbital timescales have been obtained from the Philippine Sea (Jiang et al., 2016; Seo et al., 2014; Xu et al., 2015, 2018, 2020; Wan et al., 2012) and the central equatorial Pacific (Winckler et al., 2008). In these records (Fig. 4f, g), the variability of eolian iron supply to the equatorial Pacific Ocean is shown to be well-correlated with global ice volume and with dust fluxes to Antarctica (Martínez-Garcia et al., 2011). During glacial periods, enhanced dust-borne iron fertilization of marine phytoplankton could be expected to enhance the biological pump in the Philippine Sea and the tropical Pacific more generally, which could potentially contribute to the lowering of atmospheric CO_2 concentrations (Fig. 4c). However, Winckler et al. (2016) suggested that the biological productivity was regulated by ocean dynamics, and specifically the equatorial Pacific upwelling system, which was further supported in a study of ODP Site 1240 from the eastern equatorial Pacific (Jacobel et al., 2019).

Eolian records from the mid-latitude Pacific are mostly from Shatsky Rise and Hess Rise, where sedimentation rates are higher than in the abyssal NPO. For example, core V21–146 from Shatsky Rise provides a high-resolution record of Asian dust inputs since ~500 ka (Hovan et al., 1989; Fig. 4i), revealing a clear glacial-interglacial cyclicity in the eolian dust flux. Furthermore, this record co-varies with loess-paleosol records from Xifeng (Guo et al., 2009) and Luochuan (Han et al., 2020) in the Chinese Loess Plateau (Fig. 4a, e). Increased dust fluxes during glacial intervals, suggest a direct link between strengthened loess formation and enhanced dust fluxes to the NPO. At Hess Rise, the eolian dust records in gravity core H3571 (Fig. 4h) also show higher dust fluxes during glacial intervals (Kawahata et al., 2000). In contrast, the eolian dust fluxes in core KK75–02, also from Hess Rise, show a less consistent pattern, with increases during some warm interglacials (MIS 7, 9, and 11) and decreases during certain cold glacials (e.g., MIS 6 and 14; Janecek and Rea, 1985). Meanwhile, in core SO202–37–2, also from Hess Rise, the eolian dust fluxes instead increased during interglacial periods and decreased during glacial periods (You et al., 2018). Those authors argued that the westerly winds migrated to the southern side of the Tibetan Plateau during glacials, leading to weaker winds in the more northerly Asian dust source areas, which would have restricted dust inputs to this region of the NPO. During interglacial periods, the main axis of the westerlies is proposed to have returned to the north side of the Tibetan Plateau, enabling dust inputs from the major Asian dust sources to be transported to the NPO again (You et al., 2018). Whereas the equatorial and mid-latitude Pacific sites recorded glacial-interglacial dust changes, the dust flux record in ODP Site 882 from the Subarctic North Pacific (Serno et al., 2017; Fig. 4j) is anticorrelated with summer insolation (Fig. 4n). This precession signal in the dust flux has been linked to the length of the dust season in East Asia (Serno et al., 2017). The record of black carbon from core LV76–18 also shows 23 kyr cyclicity (Cheng et al., 2022; Fig. 4k), indicated a link between precession forcing and Asian interior precipitation (Cheng et al., 2022), which could drive dust changes. In addition, based on the comparison of those records to reconstructions of marine production in the mid-latitude (Maeda et al., 2002) and subarctic Pacific Ocean (Jaccard et al., 2010; Fig. 4l, m), there is no evidence for dust-borne Fe fertilization in the high-latitude Pacific Ocean.

From the above studies, it can be concluded that there is no unified understanding of the characteristics or controlling mechanisms of eolian dust fluxes to the NPO over orbital timescales during the Quaternary period. However, in general, the orbital-scale evolution of eolian dust input to the NPO reflects paleoenvironmental changes in dust source regions (e.g., aridity, wind strength) and the northward-southward migration of the wester-

lies (Hovan et al., 1989; Janecek and Rea, 1985; Kawahata et al., 2000; You et al., 2018). Differences between records could therefore reflect the complexities in the atmospheric circulation shifts. In addition, some records could also be impacted by volcanic ash supplied by sporadic volcanism in the Kamchatka Peninsula, Kuril Islands, and Japanese island arcs, or by changes in the input of ice-rafted debris, both of which could serve to influence the reliability of dust records (Zhang et al., 2018).

4.3. Paleo-productivity in the north pacific ocean controlled by ocena dynamics

Paleo-productivity in the NPO has been intensely studied, especially in the subarctic Pacific Ocean, due to its critical impact on oceanic CO_2 storage via the biological pump (Galbraith and Skinner, 2020). Paleo-productivity changes can be inferred from primary productivity proxies (e.g., opal, total organic carbon (TOC), $CaCO_3$, Ba/Al, Si/Ti, chlorin concentration), nutrient utilization proxies (e.g., $\delta^{15}N$ and $\delta^{30}Si$), and the abundance of specific diatom species (e.g., *Chaetoceros* sp.; Brunelle et al., 2007, 2010; François et al., 1997; Galbraith et al., 2007; Galbraith and Skinner, 2020; Gray et al., 2018; Jaccard et al., 2005; Kohfeld and Chase, 2011; Max et al., 2012; Praetorius et al., 2015; Rae et al., 2014; Sigman et al., 2004: Yao et al., 2022). It should be noted that primary productivity proxies can also be influenced by preservation or diagenesis, and that dilution must be considered in records reported as the proportion of a given component rather than as accumulation rates of that component (Anderson and Winckler, 2005). In contrast, nutrient utilization proxies are generally insensitive to such factors, but they reflect the net balance between nutrient supply and productivity in the surface ocean, rather than simply recording primary productivity (Robinson et al., 2012). Enhanced nutrient utilization could reflect increased productivity, but could also reflect no change (or even a decrease) in productivity if accompanied by reduced upwelling or the supply of waters with lower nutrient content (Altieri et al., 2021). The complexity of these biological productivity proxies limits our understanding of the forcing mechanisms driving the paleo-productivity evolution in the NPO.

Previous studies of past productivity dynamics in the NPO focused on the Northern Hemisphere Glaciation (Haug et al., 1999). For example, elevated primary productivity was observed during the late Pliocene (Burls et al., 2017), whereas the intensification of Northern Hemisphere Glaciation at ~2.73 Ma led to a more permanent stratification of the water column and decreases in productivity in the subarctic Pacific Ocean (Haug et al., 1999; Sigman et al., 2004; Venti et al., 2017). In addition to the influence of ocean dynamics on primary productivity, many studies have investigated the contribution of continental iron supply to paleo-productivity changes in the subarctic Pacific Ocean, because the modern subarctic Pacific Ocean is a high-nutrient low-chlorophyll region where productivity is iron limited (Takeda, 2011). Recently, Zhang et al. (2021) provided evidence for iron fertilization of primary productivity by eolian dust before the late-Pliocene intensification of Northern Hemisphere Glaciation. Some studies have also suggested that volcanic ash from the Aleutian Arc and continental iron supplied by icebergs in the Gulf of Alaska have occasionally promoted paleo-productivity (Chen et al., 2020; Müller et al., 2018). However, as discussed in Section 4.2, eolian dust appears to have made no more than a minor contribution to productivity in the subarctic Pacific Ocean during the glacial intervals of the Quaternary period (Fig. 4; Chen et al., 2020; Jaccard et al., 2005; Knudson and Ravelo, 2015). In addition, Lembke-jene et al. (2017) suggested that iron transport from the Sea of Okhotsk by NPIW advection promoted higher primary productivity in the subarctic Pacific Ocean during the last deglaciation. However, in contrast, Lam et al. (2013) provided evidence pointing to no change in iron supply during the warm Bølling-Allerød (B-A) period, and they attributed productivity changes to physical hydrographic mechanisms. Therefore, both the nature and magnitude of the roles played by iron fertilization in the paleo-productivity of the NPO during the Quaternary period remain uncertain.

In recent years, reconstructions of primary productivity in the subarctic Pacific Ocean have mostly focused on the effect of ocean dynamics during the Last Glacial Maximum (LGM) and the deglaciation, whereas there are fewer studies on orbital timescales. Generally, higher primary productivity occurred during warm intervals such as the B-A (Gebhardt et al., 2008; Gray et al., 2018; Lam et al., 2013; Lembke-Jene et al., 2017; Maier et al., 2015; Praetorius et al., 2015) and interglacials (Brunelle et al., 2010; Galbraith et al., 2008; Jaccard et al., 2005; Kienast et al., 2004). Lower primary productivity characterized colder periods, including Heinrich Stadial 1 (HS1) and the Younger Dryas (YD) (Lembke-Jene et al., 2017; Maier et al., 2015; Rae et al., 2014), the LGM (Galbraith and Skinner, 2020; Pichevin et al., 2009), and earlier glacial intervals (Brunelle et al., 2010; Kienast et al., 2004). In general, primary productivity changes during the Quaternary have been attributed to variable exchange between the surface water and deeper interior waters, equivalently described as the formation and breakdown of near-surface stratification in the subarctic Pacific Ocean (Brunelle et al., 2007, 2010; Burls et al., 2017; Haug et al., 1999; Jaccard et al., 2005; Maier et al., 2015; Sigman et al., 2004; Studer et al., 2012).

Specifically, higher primary productivity in the NPO during warm periods has been attributed to intense wind-driven upwelling of Southern Ocean sourced deep waters, accompanied by the breakdown of NPIW stratification, which promotes the transport of major nutrients from the nutrient-rich subsurface and deep waters to the surface ocean (Brunelle et al., 2007, 2010; Burls et al., 2017; Haug et al., 1999; Maier et al., 2015). The intensified exchange between the surface and interior ocean can be explained by reduced moisture transport from low latitudes to high latitudes, due to reduced latitudinal sea surface temperature gradients during warm periods (Burls et al., 2017), and by southward movement of the westerly wind belts (Costa et al., 2018; Lawrence et al., 2013). The cold periods with lower primary productivity would have been influenced by the opposite set of processes. Such explanations for elevated productivity are consistent with active Pacific meridional overturning circulation and strong upwelling during the warm Pliocene (Burls et al., 2017; Haug et al., 1999). However, as discussed by Rae et al. (2020), the above mechanisms are hard to reconcile with the significant body of emerging evidence for enhanced NPIW formation during cold climate periods of the late Quaternary, such as the YD, HS1, and the LGM.

Hence, a contrasting view is that not only vertical but lateral transport of nutrients needs to be considered, and that intensification of NPIW formation during cold intervals such as the YD, HS1, and the LGM could have played an important role (J.W.B. Rae et al., 2020). Specifically, intensification of NPIW formation would have been associated with enhanced transport of low-nutrient subtropical surface waters to the subarctic Pacific Ocean through poleward surface currents, hence resulting in lower primary productivity at these times (Gray et al., 2018; Keigwin, 1998; Okazaki et al., 2010; Rae et al., 2014). If there was enhanced vertical mixing during cold periods such as the YD and HS1, restricted sunlight penetration could also have limited primary productivity (Lam et al., 2013; Rae et al., 2014). Enhanced North Pacific overturning could also be expected to have been associated with the transport of more saline and warmer waters from the subtropics into the subarctic Pacific Ocean during these cold periods. However, evidence from oxygen isotopes in diatoms and sea surface temperature reconstructions in cores from both the east and west subarctic Pacific Ocean suggests

there were lower sea surface temperatures and fresher surface waters at these times (Maier et al., 2015, 2018; Max et al., 2012; Riethdorf et al., 2013), in contrast to those expectations. Therefore, the existing data is equivocal and more evidence to evaluate the above hypothesis is still needed.

4.4. Modeling ocean-atmopshere coupling over the North Pacific Ocean

Both observations and climate simulations have shown that the margins of the tropics and the associated subtropical climate zones are shifting towards higher latitudes under modern climate change (Yang et al., 2020). Meanwhile, several studies have argued that the Pacific Ocean is a powerful engine for climate dynamics that exerts global impacts through atmospheric heat transport and via changes in net freshwater transport between the Pacific and Atlantic Oceans (Walczak et al., 2020; Praetorius et al., 2020). Given the limitations of proxy reconstructions and interpretations of the high-low latitude climate processes in the North Pacific, ocean-atmospheric modeling simulations are required to clarify the forcing mechanisms operating in this region, which can arise from both the ENSO and westerly wind systems.

The ENSO system is an important source of inter-annual climate variability influencing tropical ocean-atmosphere interactions. It can influence both tropical and extratropical climates through atmospheric teleconnections, including the Walker Circulation and the North Equatorial Current (Seager et al., 2019). The past evolution of the ENSO system over different timescales has been thoroughly studied through modeling approaches with varying complexities. Pioneering paleo-ENSO simulations were carried out using intermediate-complexity models, considering only a mixed-layer ocean coupled with simple atmospheric dynamics, such as the Zebiak-Cane model (Zebiak and Cane, 1987). Later, coupled general circulation models (CGCM) were implemented (Zheng et al., 2008), which can simulate the features of ENSO, such as its amplitude and spatial pattern, in greater detail (Chen et al., 2016). Recently, water isotope-enabled CGCMs have also been applied to simulate paleo-ENSO, enabling a direct model-proxy data comparison with stable isotope records (Zhu et al., 2017).

Past variations in ENSO were systematically examined in the Paleoclimate Modeling Intercomparison Project (PMIP) (Kageyama et al., 2018) for the specific periods of the mid-Holocene and the LGM, with a focus on the response of ENSO to orbital forcing (Lu and Liu, 2018), and to the expanded continental ice sheets and reduced greenhouse gas concentrations of the LGM (Lu et al., 2018). Improved computational resources have also made long continuous climate simulations feasible, and such "transient" CGCM simulations have been run to reproduce the orbital-cale evolution and abrupt changes in ENSO, such as in TRACE21 for the last 21,000 years (Liu et al., 2014; Lu et al., 2016) and in transient simulations of the last 300,000 years (Lu and Liu, 2019; Lu et al., 2019c). In these transient simulations, the time-varying changes in insolation, greenhouse gas concentrations, and continental ice sheets are taken into account. Despite model dependence, both the PMIP time-slice simulations and transient CGCM simulations reveal a qualitatively consistent weakening of ENSO towards the mid-Holocene compared to the pre-industrial. The orbital timescale evolution of ENSO intensity is suggested to be dominated by insolation forcing on the precession timescale (~21,000 years), while the forcing from greenhouse gasses and ice sheet changes over glacial-interglacial cycles tend to compensate each other and hence have only moderate effects on ENSO (Lu and Liu, 2019).

The storm tracks and westerly jet are also important features of mid-latitude climate. By transporting energy polewards, they reduce the energy imbalance between the equator and the poles (Shaw et al., 2016), thereby affecting wind strength as well as precipitation patterns. Climate model simulations demonstrate robust glacial-interglacial atmospheric-oceanic responses in the North Pacific region, highlighting the orbital-scale relationship between rainfall changes and NPIW formation in the North Pacific (Zhao et al., 2021; Fig. 5). After glacial terminations, as the summer insolation transitioned from high to low values (Fig. 5b), the modeled Northern Hemisphere westerlies responded by a northward shift (Fig. 5c). This shift-induced a shift of the North Pacific storm tracks, bringing more rainfall to the region (Fig. 5d), and in turn, the salinity of intermediate water was weakened, which may have led to the collapse of NPIW formation (Fig. 5b).

5. Future research directions

Many paleoclimatic reconstructions and modeling studies have been performed in the North Pacific open ocean and surrounding marginal seas. Several important results have been obtained, but key scientific questions remain to be solved:

(1) Reconstruction of high-resolution regional RPI stacks in the NPO. The geomagnetic field can have a non-dipolar geometry, such as during geomagnetic excursions (Roberts, 2008), whereas regional geomagnetic characteristics can be smoothed during the construction of global stacks. Hence, chronological artifacts may arise when attempting to correlate a regional RPI record in the depth domain to a global RPI reference stack in the time domain. To improve the robustness of RPI correlation, as well as to better understand regional geomagnetic field characteristics, it is essential to construct high-quality regional RPI reference stacks.

(2) Evolution of orbital-scale NPIW formation and its response to high and low latitude processes. Exploring the temporal and spatial evolution of NPIW formation, and its controlling mechanisms, will enhance our understanding of global climate forcing mechanisms in both the past and the future. Multi-dimensional NPIW information, including orientation, intensity, spatial extent, and water mass properties, should be reconstructed from marine sediment cores in the subarctic Pacific Ocean. Combining such evidence with statistical methods and paleoclimate modeling could further improve our understanding of the interrelationships between atmospheric circulation, sea ice, moisture changes, and NPIW formation, including their spatial correlation. In particular, it will be important to consider how the interactions between these components may have differed under varying climatic boundary conditions and over a range of timescales.

(3) Deciphering the controls on dust fluxes to the NPO. Both tectonic- and climate-induced changes in the source regions (e.g., tectonic uplift and aridity) and atmospheric circulation patterns across the Asian continent (e.g., the westerly circulation and the East Asian Winter Monsoon) can lead to temporal variations in provenance, flux, and grain size of dust. However, the mechanisms responsible for high dust accumulation rates in the Chinese Loess Plateau and the NPO remain controversial, with potential controls not only from source aridity but from erosion driven by monsoon precipitation or Cenozoic glaciation (Nie et al., 2018; Zhang et al., 2020a). Multi-proxy records of dust deposition from different latitudes and longitudes of the Pacific Ocean can be used to test the relationships between source region conditions, transport mechanisms, and eolian dust fluxes from the Asian interior to the Pacific Ocean, and how they have evolved through time.

(4) Patterns and drivers of subarctic Pacific primary productivity. Several studies of the last deglaciation indicate hypoxia throughout the North Pacific ocean margins and attribute this

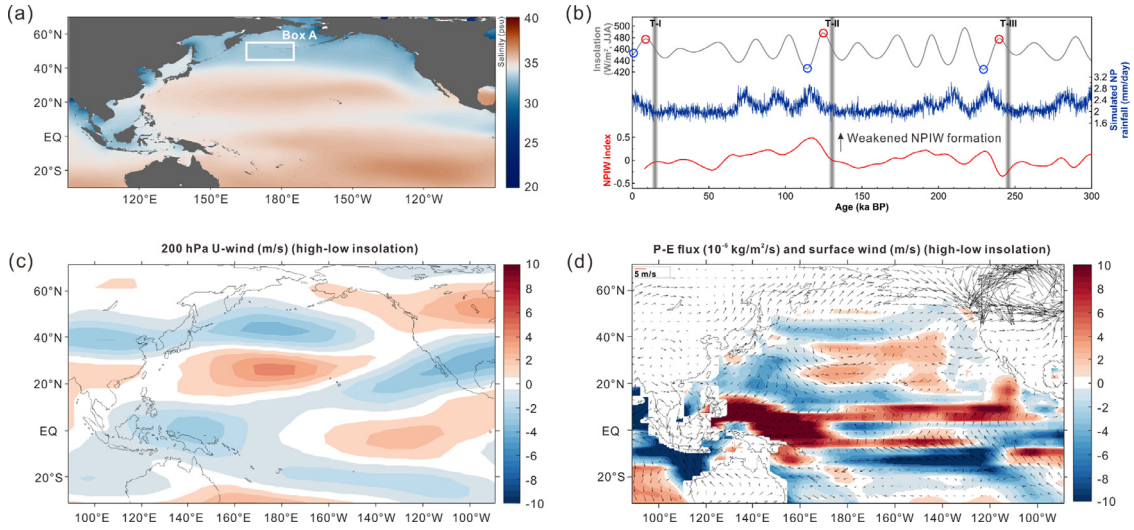

Fig. 5. Simulated atmospheric-oceanic changes in the North Pacific after glacial termination. (a) Modern sea-surface salinity in the tropical Pacific and North Pacific regions. Data from World Ocean Atlas 2018 (https://odv.awi.de/en/data/ocean/world-ocean-atlas-2018/), and map generated with Ocean Data View (http://odv.awi.de/) (Schliter, 2015). (b) Comparison of insolation forcing (JJA, gray line), simulated North Pacific rainfall in Box A (blue line), and reconstructed North Pacific Intermediate Water (NPIW) index since 300 ka (red line, higher values indicate weakened NPIW formation). (c) Map of differences in wind patterns (at 200 hPa pressure) in the North Pacific between contrasting insolation conditions (high versus low insolation) after the glacial termination. (d) Map of differences in freshwater budget (precipitation minus evaporation, P-E; color shading) and surface wind changes (arrows) in the North Pacific between those two insolation conditions. Figure adapted from Zhao et al. (2021).

phenomenon to the effects of abrupt warming and meltwater inputs (Knudson et al., 2021). However, due to spatial differences in North Pacific productivity changes between the open ocean and ocean margin settings (Iwamoto and Uematsu, 2014), the mechanisms driving productivity in this region remain elusive. Whereas major nutrients limited primary productivity during cold periods, more attention should be focused on iron sources, its potential fertilization of productivity, and its role in climate changes during relatively warm periods when primary productivity was not limited by major nutrients. In addition, more comprehensive multi-proxy studies (e.g., sea surface temperature, sea surface salinity, iron supply, primary productivity, nutrient utilization, NPIW strength), if possible within the same core, are needed to better understand the controls on primary productivity changes during glaciations and deglaciation.

(5) Model-data comparison should be expected to play a more important role in improving our understanding of North Pacific climate changes in the past and future. Long transient simulations using complex Earth system models with dynamically-simulated geochemical tracers will provide a powerful tool for future model-data comparisons. However, as models become increasingly complex, model validation will become more challenging. Since past climate records serve as a critical method for validating the models, more suitable proxy data focused on particular periods will be required. With advances in both the modeling and data approaches, an improved model-data comparison will greatly enhance our understanding of the mechanisms of North Pacific climate change and its role in the global Earth system.

Declaration of competing Interest

We declare that we have no financial and personal relationships with other people or organizations that can inappropriately influence our work, there is no professional or other personal interest of any nature or kind in any product, service and/or company that could be construed as influencing the position presented in, or the review of, the manuscript.

CRediT authorship contribution statement

Yi Zhong: Writing – original draft. **Zhengyao Lu:** Writing – review & editing. **David J. Wilson:** Writing – review & editing. **Debo Zhao:** Writing – review & editing. **Yanguang Liu:** Writing – review & editing. **Ting Chen:** Writing – review & editing. **Congcong Gai:** Writing – review & editing. **Xun Gong:** Resources. **Zhaoxia Jiang:** Resources. **Jiabo Liu:** Data curation.

Acknowledgements

The authors thank Qiang Zhang (Institute of Geology and Geophysics, Chinese Academy of Sciences) and Yanan Zhang (Southern University of Science and Technology) for helpful suggestions and modifications. The authors also thank Professor Sanzhong Li and one anonymous reviewer for their insightful input which helped us to improve the final manuscript. This work was supported financially by the Laboratory for Marine Geology, Qingdao National Laboratory for Marine Science and Technology (Nos. MGQLM-KF201818, 2022QNLM050203–3), the National Program on National Natural Science Foundation of China (grants 92158208, 41874078, 42176245, 41904069), State Key Laboratory of Marine Geology, Tongji University (No. MGK202209), the opening foundation (SSKP202101) of the Shanghai Sheshan National Geophysical Observatory (Shanghai, China), and the Shenzhen Science and Technology Program (Grant No. KQTD20170810111725321). DJW is supported by a Natural Environment Research Council independent research fellowship (NE/T011440/1).

References

Abell, J.T., Winckler, G., Anderson, R.F., Herbert, T.D., 2021. Poleward and weakened westerlies during Pliocene warmth. Nature 589, 70–75.
Altier, K.E., Fawcett, S.E., Hastings, M.G., 2021. Reactive nitrogen cycling in the atmosphere and ocean. Annu. Rev. Earth Planet. Sci. 49 (1), 523–550.
Anderson, R.F., Winckler, G., 2005. Problems with paleoproductivity proxies. Paleoceanography 20, PA3012.
Anderson, C.H., Murray, R.W., Dunlea, A.G., Giosan, L., Kinsley, C.W., McGee, D., Tada, R., 2019. Aeolian delivery to Ulleung Basin, Korea (Japan Sea), during development of the East Asian monsoon through the last 12 Ma. Geol. Mag. 157 (5), 806–817.

Bailey, I., Liu, Q., Swann, G.E.A., Jiang, Z., Sun, Y., Zhao, X., Roberts, A.P., 2011. Iron fertilisation and biogeochemical cycles in the sub-Arctic northwest Pacific during the late Pliocene intensification of northern hemisphere glaciation. Earth Planet. Sci. Lett. 307, 253–265.
Batchelor, C.L., Margold, M., Krapp, M., Murton, D.K., Dalton, A.S., Gibbard, P.L., Stokes, C.R., Murton, J.B., Manica, A., 2019. The configuration of Northern Hemisphere ice sheets through the Quaternary. Nat. Commun. 10, 3713.
Bintanja, R., van de Wal, R.S., Oerlemans, J., 2005. Modelled atmospheric temperatures and global sea levels over the past million years. Nature 437 (7055), 125–128.
Broecker, W.S., Clark, E., Hajdas, I., Bonani, G., 2004. Glacial ventilation rates for the deep Pacific Ocean. Paleoceanography 19, PA2002.
Brown, E., Colling, A., Park, D., Phillips, J., Rothery, D., Wright, J., 2001. Chapter 3-Ocean Currents Ocean Circulation. Butterworth-Heinemann, Oxford, pp. 37–78.
Brunelle, B.G., Sigman, D.M., Cook, M.S., Keigwin, L.D., Haug, G.H., Plessen, B., Schettler, G., Jaccard, S.L., 2007. Evidence from diatom-bound nitrogen isotopes for subarctic Pacific stratification during the last ice age and a link to North Pacific denitrification changes. Paleoceanogr. Paleoclimatol. 22, PA1215.
Brunelle, B.G., Sigman, D.M., Jaccard, S.L., Keigwin, L.D., Plessen, B., Schettler, G., Cook, M.S., Haug, G.H., 2010. Glacial/interglacial changes in nutrient supply and stratification in the western subarctic North Pacific since the penultimate glacial maximum. Quat. Sci. Rev. 29, 2579–2590.
Buesseler, K.O., Lamborg, C.H., Boyd, P.W., Lam, P.J., Trull, T.W., Bidigare, R.R., Bishop, J.K.B., Casciotti, K.L., Dehairs, F., Elskens, M., Honda, M., Karl, D.M., Siegel, D.A., Silver, M.W., Steinberg, D.K., Valdes, J., Van Mooy, B., Wilson, S., 2007. Revisiting carbon flux through the ocean's twilight zone. Science 316, 567–570.
Burls, N.J., Fedorov, A.V., Sigman, D.M., Jaccard, S.L., Tiedemann, R., Haug, G.H., 2017. Active Pacific meridional overturning circulation (PMOC) during the warm Pliocene. Sci. Adv. 3, e1700156.
Cavalieri, D.J., Parkinson, C.L., 1987. On the relationship between atmospheric circulation and the fluctuations in the sea ice extents of the Bering and Okhotsk Seas. J. Geophys. Res.-Oceans 92, 7141–7162.
Channell, J.E.T., Xuan, C., Hodell, D.A., 2009. Stacking paleointensity and oxygen isotope data for the last 1.5Myr (PISO-1500). Earth Planet. Sci. Lett. 283 (1), 14–23.
Channell, J.E.T., Singer, B.S., Jicha, B.R., 2020. Timing of Quaternary geomagnetic reversals and excursions in volcanic and sedimentary archives. Quat. Sci. Rev. 228, 106114.
Chen, C., Cane, M.A., Wittenberg, A.T., Chen, D.K., 2016. ENSO in the CMIP5 simulations: lifecycles, diversity, and responses to climate change. J. Clim. JCLI-D-15-0901.0901.
Chen, T., Liu, Q., Roberts, A., Shi, X., Zhang, Q., 2020. A test of the relative importance of iron fertilization from aeolian dust and volcanic ash in the stratified high-nitrate low-chlorophyll subarctic Pacific Ocean. Quat. Sci. Rev. 248, 106577.
Cheng, H., Edwards, R.L., Sinha, A., Spötl, C., Yi, L., Chen, S., Kelly, M., Kathayat, G., Wang, X., Li, X., 2016. The Asian monsoon over the past 640,000 years and ice age terminations. Nature 534, 640–646.
Cheng, T.Z., Zou, J.J., Shi, X.F., Gorbarenko, S., Vasilenko, Y., Bosin, A., Liu, Y.G., Chen, B., 2022. Climate-driven changes in high-intensity wildfire on orbital timescales in Eurasia since 320 Ka. Lithosphere 2022, 9.
Chiang, J.C.H., Fung, I.Y., Wu, C.-H., Cai, Y., Edman, J.P., Liu, Y., Day, J.A., Bhattacharya, T., Mondal, Y., Labrousse, C.A., 2015. Role of seasonal transitions and westerly jets in East Asian paleoclimate. Quat. Sci. Rev. 108, 111–129.
Costa, K.M., McManus, J.F., Anderson, R.F., 2018. Paleoproductivity and Stratification Across the Subarctic Pacific Over Glacial-Interglacial Cycles. Paleoceanogr. Paleoclimatol. 33, 914–933.
Crusius, J., Pedersen, T.F., Kienast, S., Keigwin, L., Labeyrie, L.J.G., 2004. Influence of northwest Pacific productivity on North Pacific Intermediate Water oxygen concentrations during the Bølling-Ållerød interval (14.7-12.9 ka). Geology 32, 633–636.
D'Arrigo, R., Wilson, R., Deser, C., Wiles, G., Cook, E., Villalba, R., Tudhope, A., Cole, J., Linsley, B., 2005. Tropical-North Pacific climate linkages over the past four centuries. J. Clim. 18, 5253–5265.
Davis, C.V., Myhre, S.E., Deutsch, C., Caissie, B., Praetorius, S., Borreggine, M., Thunell, R., 2020. Sea surface temperature across the Subarctic North Pacific and marginal seas through the past 20,000 years: a paleoceanographic synthesis. Quat. Sci. Rev. 246, 106519.
Ding, Q., Wallace, J.M., Battisti, D.S., Steig, E.J., Gallant, A.J.E., Kim, H.-J., Geng, L., 2014. Tropical forcing of the recent rapid Arctic warming in northeastern Canada and Greenland. Nature 509, 209–212.
Doh, S.-J., King, J.W., Leinen, M., 1988. A rock-magnetic study of giant piston core LL44-GPC3 from the central North Pacific and its paleoceanographic implications. Paleoceanography 3, 89–111.
Emile-Geay, J., Cane, M.A., Naik, N., Seager, R., Clement, A.C., Van Geen, A., 2003. Warren revisited: atmospheric freshwater fluxes and "Why is no deep water formed in the North Pacific. J. Geophys. Res. Ocean. 108 (C6), 3178.
François, R., Altabet, M.A., Yu, E.-F., Sigman, D.M., Bacon, M.P., Frank, M., Bohrmann, G., Bareille, G., Labeyrie, L.D., 1997. Contribution of Southern Ocean surface-water stratification to low atmospheric CO_2 concentrations during the last glacial period. Nature 389, 929–935.
Gai, C., Liu, Y., Shi, X., Sun, C., Jiang, X., Liu, J., Zhong, Y., Liu, Q., 2021. Recording fidelity of relative paleointensity characteristics in the North Pacific Ocean. J. Geophys. Res. 126 e2021JB022068.
Galbraith, E.D., Jaccard, S.L., Pedersen, T.F., Sigman, D.M., Haug, G.H., Cook, M., Southon, J.R., Francois, R., 2007. Carbon dioxide release from the North Pacific abyss during the last deglaciation. Nature 449, 890–893.
Galbraith, E.D., Kienast, M., Jaccard, S.L., Pedersen, T.F., Brunelle, B.G., Sigman, D.M., Kiefer, T., 2008. Consistent relationship between global climate and surface nitrate utilization in the western subarctic Pacific throughout the last 500 ka. Paleoceanogr. Paleoclimatol. 23, PA2212.
Galbraith, E.D., Skinner, L.C., 2020. The biological pump during the last glacial maximum. Ann. Rev. Mar. Sci. 12, 559–586.
Gebhardt, H., Sarnthein, M., Grootes, P.M., Kiefer, T., Kuehn, H., Schmieder, F., Röhl, U., 2008. Paleonutrient and productivity records from the subarctic North Pacific for Pleistocene glacial terminations I to V. Paleoceanography 23, PA4212.
Gong, X., Lembke-Jene, L., Lohmann, G., Knorr, G., Tiedemann, R., Zou, J.J., Shi, X.F., 2019. Enhanced North Pacific deep-ocean stratification by stronger intermediate water formation during Heinrich Stadial 1. Nat. Commun. 10, 656.
Graff, L.S., LaCasce, J.H., 2012. Changes in the extratropical storm tracks in response to changes in SST in an AGCM. J. Clim. 25, 1854–1870.
Gray, W.R., Rae, J.W.B., Wills, R.C.J., Shevenell, A.E., Taylor, B., Burke, A., Foster, G.L., Lear, C.H., 2018. Deglacial upwelling, productivity and CO_2 outgassing in the North Pacific Ocean. Nat Geosci 11, 340–344.
Guo, Z.T., Berger, A., Yin, Q.Z., Qin, L., 2009. Strong asymmetry of hemispheric climates during MIS-13 inferred from correlating China loess and Antarctica ice records. Climate Past 5 (1), 21–31.
Han, Y., Zhao, T., Song, L., Fang, X., Yin, Y., Deng, Z., Wang, S., Fan, S., 2011. A linkage between Asian dust, dissolved iron and marine export production in the deep ocean. Atmos. Environ. 45, 4291–4298.
Han, Y.M., An, Z.S., Marlon, J.R., Bradley, R.S., Zhan, C.L., Arimoto, R., Sun, Y.B., Zhou, W.J., Wu, F., Wang, Q.Y., Burr, G.S., Gao, J.J., 2020. Asian inland wildfires driven by glacial–interglacial climate change. Proc. Natl. Acad. Sci. 117 (10), 5184–5189.
Haug, G.H., Sigman, D.M., Tiedemann, R., Pedersen, T.F., Sarnthein, M., 1999. Onset of permanent stratification in the subarctic Pacific Ocean. Nature 401, 779–782.
Hays, J.D., Imbrie, J., Shackleton, N.J., 1976. Variations in the Earth's Orbit: pacemaker of the Ice ages. Science 194, 1121–1132.
Herguera, J.C., Jansen, E., Berger, W.H., 1992. Evidence for a Bathyal front at 2000-M depth in the glacial Pacific, based on a depth transect on Ontong Java Plateau. Paleoceanography 7, 273–288.
Horikawa, K., Asahara, Y., Yamamoto, K., Okazaki, Y., 2010. Intermediate Water formation in the Bering Sea during glacial periods: evidence from neodymium isotope ratios. Geology 38, 435–438.
Hovan, S.A., Rea, D.K., Pisias, N.G., Shackleton, N.J., 1989. A direct link between the China loess and marine $\delta^{18}O$ records: aeolian flux to the north Pacific. Nature 340, 296–298.
Hu, A.X., Meehl, G.A., Otto-Bliesner, B.L., Waelbroeck, C., Han, W.Q., Loutre, M.F., Lambeck, K., Mitrovica, J.X., Rosenbloom, N., 2010. Influence of Bering Strait flow and North Atlantic circulation on glacial sea-level changes. Nat. Geosci. 3, 118.
Hu, D., Wu, L., Cai, W., Sen Gupta, A., Ganachaud, A., Qiu, B., Gordon, A.L., Lin, X., Chen, Z., Hu, S., Wang, G., Wang, Q., Sprintall, J., Qu, T., Kashino, Y., Wang, F., Kessler, W.S., 2015. Pacific western boundary currents and their roles in climate. Nature 522, 299–308.
Iwamoto, Y., Uematsu, M., 2014. Spatial variation of biogenic and crustal elements in suspended particulate matter from surface waters of the North Pacific and its marginal seas. Progr. Oceanogr. 126, 211–223.
Jaccard, S.L., Galbraith, E.D., Sigman, D.M., Haug, G.H., Francois, R., Pedersen, T.F., Dulski, P., Thierstein, H.R., 2009. Subarctic Pacific evidence for a glacial deepening of the oceanic respired carbon pool. Earth Planet. Sci. Lett. 277, 156–165.
Jaccard, S.L., Haug, G.H., Sigman, D.M., Pedersen, T.F., Thierstein, H.R., Röhl, U., 2005. Glacial/interglacial changes in subarctic north pacific stratification. Science 308, 1003–1006.
Jaccard, S.L., Galbraith, E.D., Sigman, D.M., Haug, G.H., 2010. A pervasive link between Antarctic ice core and subarctic Pacific sediment records over the past 800 kyrs. Quat. Sci. Rev. 29 (1–2), 206–212.
Jacobel, A.W., Anderson, R.F., Winckler, G., Costa, K.M., Gottschalk, J., Middleton, J.L., Pavia, F.J., Shoenfelt, E.M., Zhou, Y., 2019. No evidence for equatorial Pacific dust fertilization. Nat. Geosci. 12, 154–155.
Janecek, T.R., 1985. Eolian sedimentation in the northwest Pacific Ocean: a preliminary examination of the data from deep sea drilling project sites 576 and 578. Init. Repts. DSDP 86, 589–603.
Janecek, T.R., Rea, D.K., 1983. Eolian deposition in the northeast Pacific Ocean: cenozoic history of atmospheric circulation. Geol. Soc. Am. Bull. 94, 730.
Janecek, T.R., Rea, D.K., 1985. Quaternary fluctuations in the northern hemisphere trade winds and westerlies. Quat. Res. 24, 150–163.
Jang, K., Huh, Y., Han, Y., 2017. Authigenic Nd isotope record of North Pacific Intermediate Water formation and boundary exchange on the Bering Slope. Quat. Sci. Rev. 156, 150–163.
Jiang, F.Q., Zhou, Y., Nan, Q.Y., Zhou, Y., Zheng, X.F., Li, T.G., Li, A.C., Wang, H.L., 2016. Contribution of Asian dust and volcanic material to the western Philippine Sea over the last 220 kyr as inferred from grain size and Sr-Nd isotopes. J. Geophys. Res. Ocean. 121, 6911–6928.
Jickells, T.D., An, Z.S., Andersen, K.K., Barker, A.R., Bergametti, G., Brooks, N., Cao, J.J., Boyd, P.W., Duce, R.A., Hunter, K.A., 2005. Global Iron Connections Between Desert Dust, Ocean Biogeochemistry, and Climate. Science 308 (5718), 67–71.
Kageyama, M., Braconnot, P., Harrison, S.P., Haywood, A.M., Jungclaus, J.H., Otto-Bliesner, B.L., Peterschmitt, J.-Y., Abe-Ouchi, A., Albani, S., Bartlein, P.J., Brierley, C., Crucifix, M., Dolan, A., Fernandez-Donado, L., Fischer, H., Hopcroft, P.O., Ivanovic, R.F., Lambert, F., Lunt, D.J., Mahowald, N.M., Peltier, W.R., Phipps, S.J., Roche, D.M., Schmidt, G.A., Tarasov, L., Valdes, P.J., Zhang, Q., Zhou, T., 2018. The PMIP4 contribution to CMIP6-Part 1: overview and over-arching analysis plan. Geosci. Model Dev. 11, 1033–1057.

Kawahata, H., Okamoto, T., Matsumoto, E., Ujiie, H., 2000. Fluctuations of eolian flux and ocean productivity in the mid-latitude north Pacific during the last 200 kyr. Quat. Sci. Rev. 19, 1279–1291.
Keigwin, L.D., 1998. Glacial-age hydrography of the far northwest pacific ocean. Paleoceanography 13, 323–339.
Kender, S., Aturamu, A., Zalasiewicz, J., Kaminski, M.A., Williams, M., 2019. Benthic foraminifera indicate glacial north pacific intermediate water and reduced primary productivity over bowers ridge, Bering sea, since the mid-brunhes transition. J. Micropalaeontol. 38, 177–187.
Kender, S., Ravelo, A.C., Worne, S., Swann, G.E.A., Leng, M.J., Asahi, H., Becker, J., Detlef, H., Aiello, I.W., Andreasen, D., Hall, I.R., 2018. Closure of the Bering Strait caused Mid-Pleistocene transition cooling. Nat Commun 9, 5386.
Khim, B.K., Sakamoto, T., Harada, N., 2012. Reconstruction of surface water conditions in the central region of the Okhotsk Sea during the last 180 kyrs. Deep Sea Res. Part II 61–64, 63–72.
Kiefer, T., Sarnthein, M., Erlenkeuser, H., Grootes, P.M., Roberts, A.P., 2001. North Pacific response to millennial-scale changes in ocean circulation over the last 60 kyr. Paleoceanography 16, 179–189.
Kienast, S.S., Hendy, I.L., Crusius, J., Pedersen, T.F., Calvert, S.E., 2004. Export production in the subarctic North Pacific over the Last 800 kyrs: no evidence for iron fertilization? J. Oceanogr. 60, 189–203.
King, J.W., Banerjee, S.K., Marvin, J., 1983. A new rock-magnetic approach to selecting sediments for geomagnetic paleointensity studies: application to paleointensity for the last 4000 years. J. Geophys. Res. 88, 5911–5921.
Kissel, C., Laj, C., Mulder, T., Wandres, C., Cremer, M., 2009. The magnetic fraction: a tracer of deep water circulation in the North Atlantic. Earth Planet. Sci. Lett. 288, 444–454.
Kissel, C., Van Toer, A., Laj, C., Cortijo, E., Michel, E., 2013. Variations in the strength of the North Atlantic bottom water during Holocene. Earth Planet. Sci. Lett. 369, 248–259.
Knudson, K.P., Ravelo, A.C., 2015. Enhanced subarctic Pacific stratification and nutrient utilization during glacials over the last 1.2 Myr. Geophys. Res. Lett. 42, 9870–9879.
Knudson, K.P., Ravelo, A.C., 2016. North Pacific Intermediate Water circulation enhanced by the closure of the Bering Strait. Paleoceanography 30, 1287–1304.
Knudson, K.P., Ravelo, A.C., Aiello, I.W., Knudson, C.P., Drake, M.K., Tatsuhiko, S., 2021. Causes and timing of recurring subarctic Pacific hypoxia. Sci. Adv. 7 (23), eabg2906.
Kohfeld, K.E., Chase, Z., 2011. Controls on deglacial changes in biogenic fluxes in the North Pacific Ocean. Quat. Sci. Rev. 30, 3350–3363.
Kong, W., Chiang, J.C.H., 2020. Southward shift of Westerlies intensifies the East Asian early summer rainband following El Niño. Geophys. Res. Lett. 47 (17) e2020GL088631.
Korff, L., Dobeneck, T., Frederichs, T., Kasten, S., Kuhn, G., Gersonde, R., Diekman, B., 2016. Cyclic magnetite dissolution in Pleistocene sediments of the abyssal northwest Pacific Ocean: evidence for glacial oxygen depletion and carbon trapping. Paleoceanography 31 (5), 600–624.
Kyte, F.T., Leinen, M., Heath, G.R., Zhou, L., 1993. Cenozoic sedimentation history of the central North Pacific: inferences from the elemental geochemistry of core LL44-GPC3. Geochim. Cosmochim. Acta 57, 1719–1740.
Lam, P.J., Robinson, L.F., Blusztajn, J., Li, C., Cook, M.S., Mcmanus, J.F., Keigwin, L.D., 2013. Transient stratification as the cause of the North Pacific productivity spike during deglaciation. Nat. Geosci. 6, 622–626.
Lane, C.S., Lowe, D.J., Blockley, S.P.E., Suzuki, T., Smith, V.C., 2017. Advancing tephrochronology as a global dating tool: applications in volcanology, archaeology, and palaeoclimatic research. Quat. Geochronol. 40, 1–7.
Lawrence, K.T., Sigman, D.M., Herbert, T.D., Riihimaki, C.A., Bolton, C.T., Martinez–Garcia, A., Rosell-Mele, A., Haug, G.H., 2013. Time-transgressive North Atlantic productivity changes upon Northern Hemisphere glaciation. Paleoceanography 28, 740–751.
Leduc, G., Vidal, L., Tachikawa, K., Bard, E., 2010. Changes in Eastern Pacific ocean ventilation at intermediate depth over the last 150 kyr BP. Earth Planet. Sci. Lett. 298, 217–228.
Lembke-jene, L., Tiedemann, R., Nürnberg, D., Gong, X., Lohmann, G., 2018. Rapid shift and millennial-scale variations in Holocene North Pacific intermediate water ventilation. Proc. Natl. Acad. Sci. U.S.A. 115, 5365–5370.
Lembke-Jene, L., Tiedemann, R., Nürnberg, D., Kokfelt, U., Kozdon, R., Max, L., Röhl, U., Gorbarenko, S.A., 2017. Deglacial variability in Okhotsk sea intermediate water ventilation and biogeochemistry: implications for North Pacific nutrient supply and productivity. Quat. Sci. Rev. 160, 116–137.
Leonhardt, R., Fabian, K., Winklhofer, M., Ferk, A., Laj, C., Kissel, C., 2009. Geomagnetic field evolution during the Laschamp excursion. Earth Planet. Sci. Lett. 278, 87–95.
Levi, S., Banerjee, S.K., 1976. On the possibility of obtaining relative paleointensities from lake sediments. Earth Planetary Sci. Lett. 29, 219–226.
Lisiecki, L.E., Raymo, M.E., 2005. A Pliocene-Pleistocene stack of 57 globally distributed benthic δ^{18}O records. Paleoceanography 20, PA1003.
Liu, G., Li, X., Chiang, H.-W., Cheng, H., Yuan, S., Chawchai, S., He, S., Lu, Y., Aung, L.T., Maung, P.M., Tun, W.N., Oo, K.M., Wang, X., 2020. On the glacial-interglacial variability of the Asian monsoon in speleothem δ^{18}O records. Sci. Adv. 6, eaay8189.
Liu, Z.Y., Lu, Z.Y., Wen, X.Y., Otto-Bliesner, B.L., Timmermann, A., Cobb, K.M., 2014. Evolution and forcing mechanisms of El Niño over the past 21,000 years. Nature 515, 550–553.
volume 1 Locarnini, R.A., Mishonov, A.V., Antonov, J.I., Boyer, T.P., Garcia, H.E., Baranova, O.K., Zweng, M.M., Paver, C.R., Reagan, J.R., Johnson, D.R., Hamilton, M., Seidov, D., 2013. World Ocean Atlas 2013. In: Levitus, S. (Ed.), Temperature. A. Mishonov Technical Ed.; NOAA Atlas NESDIS 73, p. 40.
Lohmann, G., Lembke-Jene, L., Tiedemann, R., Gong, X., Scholz, P., Zou, J., Shi, X., 2019. Challenges in the Paleoclimatic evolution of the arctic and subarctic pacific since the last glacial period—The Sino–German Pacific–Arctic experiment (SiGePAX). Challenges 10, 13.
Lu, N., Lohmann, G., Hinck, S., Gowan, E.J., Krebs-Kanzow, U., 2019a. The sensitivity of Northern Hemisphere ice sheets to atmospheric forcing during the last glacial cycle using PMIP3 models. J. Glaciol. 65, 645–661.
Lu, Z., Liu, Z., 2018. Examining El Nino in the Holocene: implications and challenges. Natl. Sci. Rev. 5, 807–809.
Lu, Z., Liu, Z., 2019. Orbital modulation of ENSO seasonal phase locking. Clim. Dyn. 52, 4329–4350.
Lu, Z., Liu, Z., Chen, G., Guan, J., 2019b. Prominent precession band variance in ENSO intensity over the Last 300,000 years. Geophys. Res. Lett. 46, 9786–9795.
Lu, Z., Liu, Z., Zhu, J., 2016. Abrupt intensification of ENSO forced by deglacial ice-sheet retreat in CCSM3. Clim. Dyn. 46, 1877–1891.
Lu, Z., Liu, Z., Zhu, J., Cobb, K.M., 2018. A review of paleo el nino-southern oscillation. Atmosphere (Basel) 9, 130.
Lu, Z., Miller, P.A., Zhang, Q., Warlind, D., Nieradzik, L., Sjolte, J., Li, Q., Smith, B., 2019c. Vegetation pattern and terrestrial carbon variation in past warm and cold climates. Geophys. Res. Lett. 46, 8133–8143.
Lüthi, D., Le Floch, M., Bereiter, B., Blunier, T., Barnola, J.M., Siegenthaler, U., et al., 2008. High-resolution carbon dioxide concentration record 650,000-800,000 years before present. Nature 453 (7193), 379–382.
Lyle, M., Barron, J., Bralower, T.J., Huber, M., Annette, O.L., Ravelo, A.C., Rea, D.K., et al., 2008. Pacific ocean and cenozoic evolution of climate. Rev. Geophys. 46 (2), RG2002.
Maeda, L., Kawahata, H., Nohara, M., 2002. Fluctuation of biogenic and abiogenic sedimentation on the Shatsky Rise in the western North Pacific during the late Quaternary. Mar. Geol. 189 (3), 197–214.
Maier, E., Méheust, M., Abelmann, A., Gersonde, R., Chapligin, B., Ren, J., Stein, R., Meyer, H., Tiedemann, R., 2015. Deglacial subarctic Pacific surface water hydrography and nutrient dynamics and links to North Atlantic climate variability and atmospheric CO_2. Paleoceanography 30, 949–968.
Maier, E., Zhang, X., Abelmann, A., Gersonde, R., Mulitza, S., Werner, M., Méheust, M., Ren, J., Chapligin, B., Meyer, H., Stein, R., Tiedemann, R., Lohmann, G., 2018. North Pacific freshwater events linked to changes in glacial ocean circulation. Nature 559, 241–245.
Martin, J.H., 1990. Glacial-interglacial CO_2 change: the Iron Hypothesis. Paleoceanography 5, 1–13.
Martínez-Garcia, A., Rosell-Melé, A., Jaccard, S.L., Geibert, W., Sigman, D.M., Haug, G.H., 2011. Southern Ocean dust–climate coupling over the past four million years. Nature 476 (7360), 312–315.
Matsumoto, K., Oba, T., Lynch-Stieglitz, J., Yamamoto, H., 2002. Interior hydrography and circulation of the glacial Pacific Ocean. Quat. Sci. Rev. 21, 1693–1704.
Max, L., Riethdorf, J.R., Tiedemann, R., Smirnova, M., Mollenhauer, G., 2012. Sea surface temperature variability and sea-ice extent in the subarctic northwest Pacific during the past 15,000 years. Paleoceanography 27, PA3213.
Max, L., Lembke-Jene, L., Riethdorf, J.R., Tiedemann, R., Nürnberg, D., Kühn, H., Mackensen, A., 2014. Pulses of enhanced North Pacific Intermediate Water ventilation from the Okhotsk Sea and Bering Sea during the last deglaciation. Climate Past 10 (2), 591–605.
Max, L., Rippert, N., Lembke-Jene, L., Mackensen, A., Nürnberg, D., Tiedemann, R., 2017. Evidence for enhanced convection of North Pacific Intermediate Water to the low-latitude Pacific under glacial conditions. Paleoceanogr. Paleoclimatol. 32 (1), 41–55.
Müller, J., Romero, O., Cowan, E.A., Mcclymont, E.L., Forwick, M., Asahi, H., März, C., Moy, C.M., Suto, I., Mix, A., 2018. Cordilleran ice-sheet growth fueled primary productivity in the Gulf of Alaska, northeast Pacific Ocean. Geology 46.
Nichols, M.D., Xuan, C., Crowhurst, S., Hodell, D.A., Richter, C., Acton, G.D., Wilson, P.A., 2020. Climate-induced variability in mediterranean outflow to the North Atlantic ocean during the late pleistocene. Paleoceanogr. Paleoclimatol. 35 (9) e2020PA003947.
Nie, J.S., Pullen, A., Garzione, C.N., Peng, W.B., Wang, Z., 2018. Pre-Quaternary decoupling between Asian aridification and high dust accumulation rates. Sci. Adv. 4 (2), eaao6977.
Okazaki, Y., Sagawa, T., Asahi, H., Horikawa, K., 2012. Ventilation changes in the western North Pacific since the last glacial period. Climate Past 8, 17–24.
Okazaki, Y., Timmermann, A., Menviel, L., Harada, N., Abe-Ouchi, A., Chikamoto, M.O., Mouchet, A., Asahi, H., 2010. Deepwater formation in the North Pacific during the last glacial termination. Science 329, 200–204.
Ovsepyan, E., Ivanova, E., Tetard, M., Max, L., Tiedemann, R., 2021. Intermediate- and Deep-water oxygenation history in the subarctic north pacific during the last deglacial period. Front. Earth Sci. 9, 638069.
Patterson, D.B., Farley, K.A., Norman, M.D., 1999. ^{4}He as a tracer of continental dust: a 1.9 million year record of aeolian flux to the west equatorial Pacific Ocean. Geochim. Cosmochim. Acta 63, 615–625.
Pichevin, L.E., Reynolds, B.C., Ganeshram, R.S., Cacho, I., Pena, L., Keefe, K., Ellam, R.M.J.N., 2009. Enhanced carbon pump inferred from relaxation of nutrient limitation in the glacial ocean. Nature 459, 1114–1117.
Praetorius, S.K., Mix, A.C., Walczak, M.H., Wolhowe, M.D., Addison, J.A., Prahl, F.G., 2015. North Pacific deglacial hypoxic events linked to abrupt ocean warming. Nature 527, 362.
Praetorius, S.K., Condron, A., Mix, A.C., Walczak, M.H., Mckay, J.L., Du, J.H., 2020. The role of Northeast Pacific meltwater events in deglacial climate change. Sci Adv 6 (9), eaay2915.

Qiu, B., 2002. Large-scale variability in the Midlatitude subtropical and subpolar north pacific ocean: observations and causes. J. Phys. Oceanogr 32, 353–375.
Rae, J.W.B., Gray, W.R., Wills, R.C.J., Eisenman, I., Fitzhugh, B., Fotheringham, M., Littley, E.F.M., Rafter, P.A., Rees-Owen, R., Ridgwell, A., Taylor, B., Burke, A., 2020. Overturning circulation, nutrient limitation, and warming in the. Glacial North Pacific. Sci. Adv. 6, eabd1654.
Rae, J.W.B., Sarnthein, M., Foster, G.L., Ridgwell, A., Grootes, P.M., Elliott, T., 2014. Deep water formation in the North Pacific and deglacial CO_2 rise. Paleoceanography 29, 645–667.
Rea, D.K., Janecek, T.R., 1981. Mass-accumulation rates of the non-authigenic inorganic crystalline (eolian) component of deep-sea sediments from the western Mid Pacific Mountains, Deep Sea Drilling Project Site 463. Initial Report. Deep Sea Drill. Proj. 62, 653–659.
Rea, D.K., Snoeckx, H., Joseph, L.H., 1998. Late Cenozoic Eolian deposition in the North Pacific: asian drying, Tibetan uplift, and cooling of the northern hemisphere. Paleoceanography 13, 215–224.
Rella, S.F., Tada, R., Nagashima, K., Ikehara, M., Itaki, T., Ohkushi, K.I., Sakamoto, T., Harada, N., Uchida, M.J.P., 2012. Abrupt changes of intermediate water properties on the northeastern slope of the Bering Sea during the last glacial and deglacial period. Paleoceanography 27, PA3203.
Riethdorf, J.R., Max, L., Nürnberg, D., Lembke-Jene, L., Tiedemann, R.J.P., 2013. Deglacial development of (sub) sea surface temperature and salinity in the subarctic northwest Pacific: implications for upper-ocean stratification. Paleoceanography 28, 91–104.
Roberts, A.P., 2008. Geomagnetic excursions: knowns and unknowns. Geophys. Res. Lett. 35, L17307.
Roberts, A.P., 2015. Magnetic mineral diagenesis. Earth Sci. Rev. 151, 1–47.
Roberts, A.P., Lehman, B.T., Weeks, R.J., Verosub, K.L., Laj, C., 1997. Relative paleointensity of the geomagnetic field over the last 200,000 years from ODP Sites 883 and 884, North Pacific Ocean. Earth Planetary Sci. Lett. 152, 11–23.
Roberts, A.P., Tauxe, L., Heslop, D., 2013. Magnetic paleointensity stratigraphy and high-resolution Quaternary geochronology: successes and future challenges. Quat. Sci. Rev. 61, 1–16.
Robinson, R.S., Kienast, M., Albuquerque, A.L., Altabet, M., Contreras, S., Holz, R.D.P., Dubois, N., Francois, R., Galbraith, E., Hsu, T.C., 2012. A review of nitrogen isotopic alteration in marine sediments. Paleoceanography 27 (4), 89–108.
Sakamoto, T.T., Hasumi, H., Ishii, M., Emori, S., Suzuki, T., Nishimura, T., Sumi, A., 2005. Responses of the Kuroshio and the Kuroshio Extension to global warming in a high-resolution climate model. Geophys. Res. Lett. 32, L14617.
Scheff, J., Frierson, D., 2012. Twenty-first-century Multimodel subtropical precipitation declines are mostly Midlatitude shifts. J Clim 25, 4330–4347.
Schlitzer, R., 2015. Ocean data view. http://odv.awi.de.
Seager, R., Cane, M., Henderson, N., Lee, D.E., Abernathey, R., Zhang, H.H., 2019. Strengthening tropical Pacific zonal sea surface temperature gradient consistent with rising greenhouse gases. Nat. Clim. Chang. 9 (7), 517–522.
Serno, S., Winckler, G., Anderson, R.F., Jaccard, S.L., Kienast, S.S., Haug, G.H., 2017. Change in dust seasonality as the primary driver for orbital-scale dust storm variability in East Asia. Geophys. Res. Lett. 44, 3796–3805.
Seo, I., Lee, Y.I., Yoo, C.M., Kim, Y.J., Hyeong, K., 2014. Sr-Nd isotope composition and clay mineral assemblages in eolian dust from the central Philippine Sea over the last 600 kyr: implications for the transport mechanism of Asian dust. J. Geophys. Res. 119 (19), 11492–11504.
Shao, Y., Wyrwoll, K.-H., Chappell, A., Huang, J., Lin, Z., McTainsh, G.H., Mikami, M., Tanaka, T.Y., Wang, X., Yoon, S., 2011. Dust cycle: an emerging core theme in Earth system science. Aeolian Res. 2, 181–204.
Shaw, T.A., Baldwin, M., Barnes, E.A., Caballero, R., Garfinkel, C.I., Hwang, Y.T., Li, C., O'Gorman, P.A., Rivière, G., Simpson, I.R., Voigt, A., 2016. Storm track processes and the opposing influences of climate change. Nat. Geosci. 9, 656–664.
Shcherbina, A.Y., Talley, L.D., Rudnick, D.L., 2003. Direct obsercations of North Pacific ventilation: brine rejection in the Okhotsk Sea. Science 302 (5652), 1952–1955.
Shen, X.Y., Wan, S.M., France-Lanord, C., Clift, P.D., Tada, R., Révillon, S., Shi, X.F., Zhao, D.B., Liu, Y.G., Yin, X.B., Song, Z.H., Li, A.C., 2017. History of Asian eolian input to the Sea of Japan since 15 Ma: links to Tibetan uplift or global cooling? Earth Planet. Sci. Lett. 474, 296–308.
Shin, J.Y., Yu, Y., Seo, I., Hyeong, K., Lim, D., Kim, W., 2018. Magnetic properties of deep-sea sediments from the North Pacific: a proxy of glacial deep-water ventilation. Geochem. Geophys. Geosyst. 19 2018GC007735.
Shin, J.Y., Yu, Y., Kim, W., 2019. Wavelet-based verification of a relative paleointensity record from the North Pacific. Earth, Planets Space 71, 88.
Sigman, D.M., Hain, M.P., Haug, G.H., 2010. The polar ocean and glacial cycles in atmospheric CO_2 concentration. Nature 466, 47–55.
Sigman, D.M., Jaccard, S.L., Haug, G.H., 2004. Polar ocean stratification in a cold climate. Nature 428, 59.
Simon, Q., Thouveny, N., Bourlès, D.L., Nuttin, L., Hillaire-Marcel, C., St-Onge, G., 2016. Authigenic $^{10}Be/^{9}Be$ ratios and ^{10}Be-fluxes ($^{230}Thxs$-normalized) in central Baffin Bay sediments during the last glacial cycle: paleoenvironmental implications. Quat. Sci. Rev. 140, 142–162.
Studer, A.S., Martínez-Garcia, A., Jaccard, S.L., Girault, F.E., Sigman, D.M., Haug, G.H., 2012. Enhanced stratification and seasonality in the Subarctic Pacific upon Northern Hemisphere Glaciation–New evidence from diatom-bound nitrogen isotopes, alkenones and archaeal tetraethers. Earth Planet. Sci. Lett. 351-352, 84–94.
Sun, Y.B., Yan, Y., Nie, J.S., Li, G.J., Shi, Z.G., Qiang, X.K., Chang, H., An, Z.S., 2019. Source-to-sink fluctuations of Asian eolian deposits since the late Oligocene. Earth Sci. Rev. 200, 102963.
Takeda, S., 2011. Iron and phytoplankton growth in the subarctic North Pacific. Aqua-BioSci. Monogr. 4, 41–93.
Talley, L.D., 2003. Shallow, intermediate, and deep overturning components of the global heat budget. J. Phys. Oceanogr. 101 (C9), 20869–20876.
Talley, L.D., 2013. Closure of the global overturning circulation through the indian, pacific, and southern oceans: schematics and transports. Oceanography 26 (1), 80–97.
Tanaka, S., Takahashi, K., 2005. Late Quaternary paleoceanographic changes in the Bering Sea and the western subarctic Pacific based on radiolarian assemblages. Deep Sea Research Part II Topical Studies in Oceanography 52, 2131–2149.
Tauxe, L., 1993. Sedimentary records of relative paleointensity of the geomagnetic field: theory and practice. Rev. Geophys. 31, 319–354.
Tauxe, L., Steindorf, J.L., Harris, A., 2006. Depositional remanent magnetization: toward an improved theoretical and experimental foundation. Earth Planet. Sci. Lett. 244, 515–529.
Vats, N., Mishra, S., Singh, R.K., Gupta, A.K., Pandey, D.K., 2020. Paleoceanographic changes in the East China Sea during the last ~400 kyr reconstructed using planktic foraminifera. Glob. Planet Change 189, 103173.
Venti, N., Billups, K., Herbert, T., 2017. Paleoproductivity in the northwestern Pacific Ocean during the Pliocene-Pleistocene climate transition (3.0-1.8 Ma): site 1208 paleoproductivity. Paleoceanography 32, 92–103.
Wan, S., Li, A., Clift, P.D., Stuut, J.-B.W., 2007. Development of the East Asian monsoon: mineralogical and sedimentologic records in the northern South China Sea since 20 Ma. Palaeogeogr. Palaeoclimatol. Palaeoecol. 254, 561–582.
Wan, S.M., Sun, Y.B., Nagashima, K., 2020. Asian dust from land to sea: processes, history and effect from modern observation to geological records. Geol. Mag. 157 (5), 701–706.
Walczak, M.H., Mix, A.C., Cowan, E.A., Fallon, S., Fifield, L.K., Alder, J.R., Du, J.H., Haley, B., Hobern, T., Padman, J., Praetorius, S.K., Schmittner, A., Stoner, J.S., Zellers, S.D., 2020. Phasing of millennial-scale climate variability in the Pacific and Atlantic Oceans. Science 370 (6517), 716–720.
Wan, S.M., Yu, Z.J., Clift, P.D., Sun, H.J., Li, A.C., Li, T.G., 2012. History of Asian eolian input to the West Philippine Sea over the last one million years. Palaeogeogr. Palaeoclimatol. Palaeoecol. 326-328, 152–159.
Wang, W.Z., Tilo, v.D., Frederichs, T., Zhang, Y., Lembke-Jene, L., Tiedemann, R., Winklhofer, M., Nürnberg, D., 2021. Dating North Pacific abyssal sediments by geomagnetic paleointensity: implications of magnetization carriers, plio-pleistocene climate change, and benthic redox conditions. Front. Earth Sci. 9 (577), 683177.
Wang, Y., Cheng, H., Edwards, R.L., Kong, X., Shao, X., Chen, S., Wu, J., Jiang, X., Wang, X., An, Z., 2008. Millennial- and orbital-scale changes in the East Asian monsoon over the past 224,000 years. Nature 451, 1090–1093.
Warren, B.A., 1983. Why is no deep water formed in the North Pacific? J. Mar. Res. 41, 327–347.
Weber, E.T., Owen, R.M., Dickens, G.R., Halliday, A.N., Jones, C.E., Rea, D.K., 1996. Quantitative resolution of eolian continental crustal material and volcanic detritus in North Pacific surface sediment. Paleoceanography 11, 115–127.
Winckler, G., Anderson, R.F., Feisher, M.Q., Mcgee, D., Mahowald, N., 2008. Covariant glacial-interglacial dust fluxes in the equatorial Pacific and Antarctica. Science 320 (5872), 93.
Winckler, G., Anderson, R.F., Jaccard, S.L., Marcantonio, F., 2016. Ocean dynamics, not dust, have controlled equatorial Pacific productivity over the past 500,000 years. Proc. Natl. Acad. Sci. U.S.A. 113, 6119.
Worne, S., Kender, S., Swann, G.E.A., Leng, M.J., Ravelo, A.C., 2019. Coupled climate and subarctic Pacific nutrient upwelling over the last 850,000 years. Earth Planet. Sci. Lett. 522, 87–97.
Wu, B., Wang, J., 2002. Winter arctic oscillation, siberian high and east asian winter monsoon. Geophys. Res. Lett. 29 3-1.
Xu, Z.K., Li, T.G., Clift, P.D., Lim, D., Wan, S.M., Chen, H.J., Tang, Z., Jiang, F.Q., Xiong, Z.F., 2015. Quantitative estimates of Asian dust input to the western Philippine Sea in the mid-late Quaternary and its potential significance for paleoenvironment. Geochem. Geophysic. Geosystem. 16 (9), 3182–3196.
Xu, Z.K., Li, T.G., Clift, P.D., Wan, S.M., Qiu, X.H., Lim, D., 2018. Bathyal records of enhanced silicate erosion and weathering on the exposed Luzon shelf during glacial lowstands and their significance for atmospheric CO_2 sink. Chem. Geol. 476, 302–315.
Xu, Z.K., Wan, S.M., Colin, C., Li, T.G., Chang, F.M., Sun, R.T., Yu, Z.J., Lim, D., 2020. Enhanced terrigenous organic matter input and productivity on the western margin of the Western Pacific Warm Pool during the Quaternary sea-level lowstands: forcing mechanisms and implications for the global carbon cycle. Quat. Sci. Rev. 232, 106211.
Yamamoto, Y., Yamazaki, T., Kanamatsu, T., Ioka, N., Mishima, T., 2007. Relative paleointensity stack during the last 250 kyr in the northwest Pacific. J. Geophys. Res. Atmospher. 112, 534–535.
Yamazaki, T., 1999. Relative paleointensity of the geomagnetic field during Brunhes Chron recorded in North Pacific deep-sea sediment cores: orbital influence? Earth Planet. Sci. Lett. 169, 23–35.
Yamazaki, T., Ioka, N., 1997a. Cautionary note on magnetic grain-size estimation using the ratio of ARM to magnetic susceptibility. Geophys. Res. Lett. 24, 751–754.
Yamazaki, T., Ioka, N.J.P., 1997b. Environmental rock-magnetism of pelagic clay: implications for Asian Eolian input to the North Pacific since the Pliocene. 12, 111–124.
Yamazaki, T., Shimono, T., 2013. Abundant bacterial magnetite occurrence in oxic red clay. Geology 41, 1191–1194.
Yamazaki, T., Shimono, T., Inoue, S., 2016. Paleomagnetic inclination variations during the last 200 kyr in the Okhotsk Sea and their relation to persistent non-axial-dipole field. Earth Planets Space 68, 174.

Yang, H., Lohmann, G., Krebs-Kanzow, U., Ionita, M., Shi, X., Sidorenko, D., Gong, X., Chen, X., Gowan, E.J., 2020. Poleward shift of the major ocean gyres detected in a warming climate. Geophys Res Lett 47 e2019GL085868.
Yan, Y., Ma, L., Sun, Y.B., 2017. Tectonic and climatic controls on provenance changes of fine-grained dust on the Chinese Loess Plateau since the late Oligocene. Geochim. Cosmochim. Acta 200, 110–122.
Yao, Z.Q., Liu, Y.G., Shi, X.F., Gong, X., Gorbarenko, S.A., Bosin, A.A., Gao, J.J., Bai, Y.Z., Zhang, H., Wang, A.Q., 2022. Paleoproductivity variations and implications in the subarctic northwestern Pacific since MIS 7: geochemical evidence. Glob. Planet Change 209, 103730.
Yi, L., Xu, D., Jiang, X.Y., Ma, X.L., Ge, Q., Deng, X.G., Wang, H.F., Deng, C.L., 2020. Magnetostratigraphy and Authigenic 10Be/9Be dating of plio-pleistocene abyssal surficial sediments on the southern slope of mariana trench and sedimentary processes during the mid-pleistocene transition. J, Geophys. Res.: Ocean 125 (8) e2020JC016250.
You, D.F., Wang, R.J., Xiao, W.S., 2018. Correlations between biogenic components and dust input and their change mechanism on Hess Rise, Central North Pacific during the Late Quaternary. Adv. Earth Sci. 33 (11), 1203–1214.
Yuan, X., Talley, L.D., 1996. The subarctic frontal zone in the North Pacific: characteristics of frontal structure from climatological data and synoptic surveys. J. Geophys. Res. Ocean. 101, 16491–16508.
Zebiak, S.E., Cane, M.A., 1987. A model El Niño-southern oscillation. Month. Weather Rev. 115 (10), 2262–2278.
Zhang, Q., Liu, Q.S., Li, J., Sun, Y., 2018. An integrated study of the eolian dust in pelagic sediments from the North Pacific Ocean based on environmental magnetism, transmission electron microscopy and diffuse reflectance spectroscopy. J. Geophys. Res. Solid Earth 122, 3358–3376.
Zhang, Q., Liu, Q.S., Sun, Y.B., 2020b. Review of recent developments in aeolian dust signals of sediments from the North Pacific Ocean based on magnetic minerals. Geol. Mag. 157, 790–805.
Zhang, Q., Liu, Q.S., Roberts, A.P., Larrasoaña, J.C., Shi, X., Jin, C., 2020a. Mechanism for enhanced eolian dust flux recorded in North Pacific Ocean sediments since 4.0 Ma: aridity or humidity at dust source areas in the Asian interior? Geology 48, 77–81.
Zhang, Q., Liu, Q.S., Roberts, A.P., Yu, J.M., Liu, Y., Li, J.H., 2021. Magnetotactic Bacterial Activity in the north pacific ocean and its relationship to asian dust inputs and primary productivity since 8.0 Ma. Geophys. Res. Lett. 48 (15) e2021GL094687.
Zhang, W.F., Li, G.J., Chen, J., 2019. The application of Neodymium isotope as a chronostratigraphic tool in North Pacific sediments. Geol. Mag. 157 (5), 768–776.
Zhang, Y., Huang, D., 2011. Has the East Asian westerly jet experienced a poleward displacement in recent decades? Adv. Atmosphere Sci. 28, 1259–1265.
Zhao, D., Wan, S., Lu, Z., Zhai, L., Feng, X., Shi, X., Li, A., 2021. Delayed collapse of the north pacific intermediate water after the glacial termination. Geophys. Res. Lett. 48 e2021GL092911.
Zheng, W., Braconnot, P., Guilyardi, E., Merkel, U., Yu, Y., 2008. ENSO at 6ka and 21ka from ocean-atmosphere coupled model simulations. Clim. Dyn. 30, 745–762.
Zheng, X.F., Kao, S.J., Chen, Z., Menviel, L., Chen, H., Du, Y., Wan, S.M., Yan, H., Liu, Z.H., Zheng, L.W., 2016. Deepwater circulation variation in the South China Sea since the last glacial maximum. Geophys. Res. Lett. 43 (16), 8590–8599.
Zhong, Y., Liu, Y., Gong, X., Wilson, D.J., Lu, Z., Liu, J., Song, T., Gorbarenko, S.A., Shi, X., Yang, X., Liu, Q., 2021. Coupled impacts of atmospheric circulation and sea-ice on late pleistocene terrigenous sediment dynamics in the subarctic pacific ocean. Geophys. Res. Lett. 48 e2021GL095312.
Zhong, Y., Liu, Y., Yang, X., Zhang, J., Liu, J., Bosin, A., Gorbarenko, S.A., Shi, X., Chen, T., Chou, Y.-.M., Liu, W., Wang, H., Gai, C., Liu, J., Derkachev, A.N., Qiang, X., Liu, Q., 2020. Do non-dipole geomagnetic field behaviors persistently exist in the subarctic Pacific Ocean over the past 140 ka? Sci. Bull. 65, 1505–1507.
Zhu, J., Liu, Z., Brady, E., Otto-Bliesner, B., Zhang, J., Noone, D., Tomas, R., Nusbaumer, J., Wong, T., Jahn, A., Tabor, C., 2017. Reduced ENSO variability at the LGM revealed by an isotope-enabled Earth system model. Geophys Res Lett 44, 6984–6992.
Ziegler, C.L., Murray, R.W., 2007. Geochemical evolution of the central Pacific ocean over the past 56Myr. Paleoceanography 22, 162–179.
Zou, J., Chang, Y.-.P., Zhu, A., Chen, M.-.T., Kandasamy, S., Yang, H., Cui, J., Yu, P.-.S., Shi, X., 2021. Sedimentary mercury and antimony revealed orbital-scale dynamics of the Kuroshio current. Quat. Sci. Rev. 265, 107051.